Department of Pharmacy, Faculty of Health Sciences
UiT – The Arctic University of Norway

Isolation, characterization and chondrogenic differentiation of adult stem cell-derived MUSE-cells

—

Lars-Arne Johansen
Supervisor: Professor Inigo Zubiavrre Martinez
Thesis for the degree Master of Pharmacy, May 2016

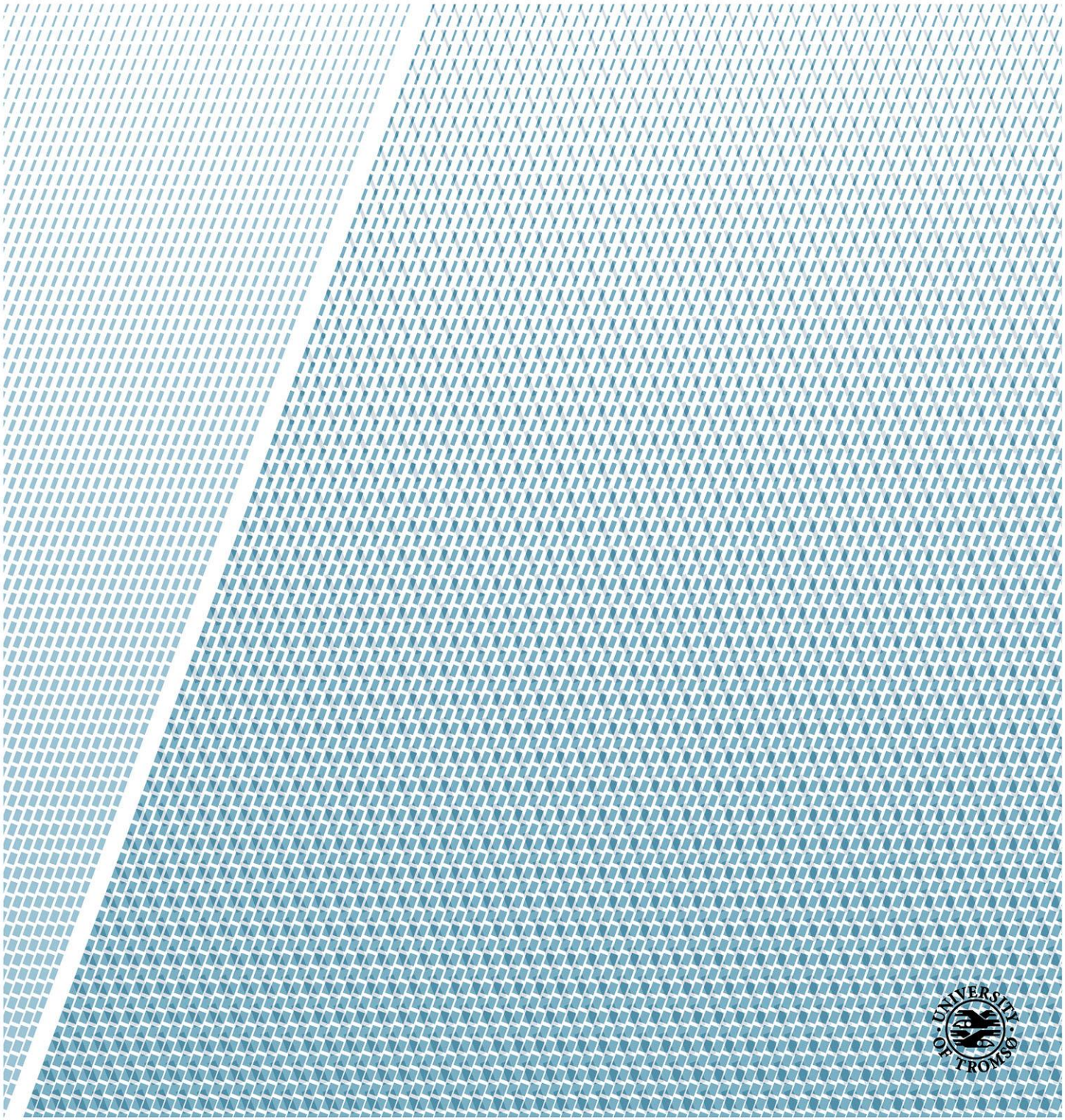

Summary

Articular cartilage is coating the layers of freely movable joints, enabling a smooth surface and acts resisting to forces. The tissue is aneural and avascular, and has a poor ability to self-renew in cases of tissue damage. Therefore, cartilage lesions often lead to degenerative disorders such as osteoarthritis (OA). OA is considered the most common form of arthritis affecting people worldwide, causing pain and physical disability. Approaches in cartilage regeneration, especially the use of mesenchymal stem cells (MSCs), have been promising, yet limited. Finding a the most suitable cell type for transplantation strategies is still matter of debate. The recent discovery of a pluripotent stem cell type that represent a minor fraction of the stromal cells present in tissues (MUSE-cells) offer an attractive alternative that deserve to be investigated.

The main objective of this study was to establish protocols for the isolation and characterization of MUSE-cells from Hoffa's fat pad (HFP) and umbilical cords (MC), and to compare the chondrogenic differentiation potential between the MUSE- and non-MUSE-cell populations. MUSE-cells were isolated from the total pull of mesenchymal stem cells by cell sorting, using the embryonic marker SSEA-3 as specific cell surface antigen. Scaffold-free 3D cultures maintained in chondrogenic conditions were used to induce cartilage differentiation. Single cell cluster formation assays were used for functional characterization of MUSE. Pluripotent NTERA-2 cells were used as positive control.

Mesenchymal cells displaying phenotypic characteristics of stem cells (MSCs) were successfully isolated from fresh tissues. Scaffold-free spheroids of HFP-MSCs showed a more intense Alcian blue (matrix) staining and had better cartilage-like morphology than those formed from mixed cord MSCs (MC-MSCs). SSEA-3^{+} MUSE-cells could be identified and isolated from HFP (8% of total MSCs) but were nearly undetectable in MC (0.8% of total MSCs). Phenotypic characterization of sorted cells after cell expansion, and functional characterization by single cell cluster formation abilities confirmed the pluripotent nature of the cells.

We have demonstrated that the adipose tissue of the infrapatellar pocket (HFP) is a good source of MSCs, with the ability to produce cartilage-like spheroids, and contain a fraction of SSEA-3^+ cells (MUSE-cells) with the ability to self-renew. This cell subtype was also highly positive for the pluripotency marker SSEA-4. MC-MSCs on the other hand, did not manage to produce spheroids with properties similar to those of native cartilage, and had not SSEA-3^+ MUSE-cells. The chondrogenic abilities of MUSE- and non-MUSE-cells from HFP is under investigation at the time of writing this thesis.

Keywords: Articular cartilage, Articular cartilage disorders, Multilineage-differentiating stress enduring (MUSE) cells, Regenerative medicine, Hoffa's fat pad, Umbilical cord, Chondrogenesis, Mesenchymal stem cells, SSEA-3, SSEA-4, Cell sorting.

Acknowledgements

This master project was carried out at the Department of Bone and Joint Research Group at Institute of Clinical Medicine, University of Tromsø (UiT) – The Arctic University of Norway.

First and foremost, I would like to express my deepest gratitude to my supervisor, Professor Inigo Zubiavrre Martinez. There are no words to describe my appreciation of your help to keep me on track, including the time you have put into helping me. Thank you for introducing me to the world of science and for sharing your knowledge with me. It has been an honor to participate in this novel field of stem cell research.

Further, I will send my regards to Ph.D. candidate Ashraful Islam. Thank you for all you have taught me about laboratory work and for helping me cross my personal boundaries within this field. Also, thank you for sharing your knowledge with me. I will also like to acknowledge engineer Kirsti Rønne and Dr. Ann Kristin Hansen, always willing to help. I am very grateful of the way your research group have accepted me, with open arms.

I want to thank my mom and dad for supporting me all the way through these five years of studying. My graduation would not have been possible without you. I also want to thank my aunt, Signy Bendiksen, for helping me choose this area of study five years ago. This has been an important decision in my life. I also want to thank my friends for helping me keep my spirits up and supporting me throughout this period. Thanks to the Pharmacy class of 2011 and all the other fantastic people at the Department of Pharmacy for always providing a nice social environment. And thanks to you, Edmund Theodore Assignon, for being a second reader of this thesis. I am gratefully indebted to your valuable comments.

Lars-Arne Johansen

May 2016

Abbreviations

α-MEM	Minimum Essential Medium Eagle, alpha modification
AA	Ascorbic Acid
AC	Articular cartilage
ACI	Autologous chondrocyte implantation
ADAMTS	A Disintegrin And Metalloproteinase with Thrombospondin Motifs
ALP	Alkaline phosphatase
AMIC	Autologous Matrix Induced Chondrogenesis
ASC	Adult stem cell
AT	Adipose tissue
AT-MSCs	Adipose tissue derived mesenchymal stem cells
bFGF	Basic fibroblast growth factor
BM	Bone marrow
BM-HSC	Bone marrow hematopoietic stem cell
BM-MSC	Bone marrow mesenchymal stem cell
BME	Basal Medium Eagle
BMP-2	Bone Morphogenetic Protein-2
BSA	Bovine serum albumin
CACI	Collagen-membrane cover ACI
CD	Cluster of differentiation
C.W.	Conical Well
DEX	Dexamethasone
DMEM	Dulbecco's modified eagle's medium
DMSO	Dimethyl Sulfoxide
EC	Embryonic carcinoma
ECM	Extracellular matrix
EDTA	Ethylenediaminetetraacetic acid
ESC	Embryonic stem cell
EtOH	Ethanol

FACS	Fluorescence-activated cell sorting
FBS	Fetal Bovine Serum
FDA	Food and Drug Administration
FITC	Fluorescein isothiocyanate
GAG	Glycosaminoglycan
GvHD	Graft-versus-host disease
HA	Hyaluronic acid
H.D.	Hanging Drop
HFP	Hoffa's Fat Pad
HFP-MSCs	Hoffa's Fat Pad derived mesenchymal stem cells
hMSCs	Human mesenchymal stem cells
HSA	Human serum albumin
HSC	Hematopoietic stem cell
IFP	Infrapatellar Fat Pad
IL-1	Interleukin 1
iPSC	Induced pluripotent stem cell
ITS	Insulin-Transferrin-Selenium
JIA	Juvenile idiopathic arthritis
LBP	Low binding plate
LTT	Long-term trypsin incubation
M-cluster	MUSE-cell derived cluster
MACI	Matrix-induced autologous chondrocyte implantation
MC	Mixed Cord
MC-MSCs	Mixed Cord derived mesenchymal stem cells
MEC	MUSE Enriched Cell cultures
MMP	Matrix metallo-proteinase
MSC	Mesenchymal stem cell
MUSE-cell	Multilineage differentiating stress-enduring cell
OA	Osteoarthritis

PBS	Phosphate buffered saline
Poly-HEMA	Poly (2-hydroxyethyl methacrylate)
P/S	Penicillin and Streptomycin
RA	Rheumatoid arthritis
SCST	Severe cellular stress treatment
SM	Synovial membrane
SM-MSCs	Synovial membrane derived mesenchymal stem cells
SSEA-3	Stage-specific Embryonic Antigen-3
SSEA-4	Stage-specific Embryonic Antigen-4
TGF-β	Transforming growth factor beta
TNF-α	Tumor necrosis factor alpha
UC	Umbilical cord
UCB	Umbilical cord blood
UC-MSCs	Umbilical cord derived mesenchymal stem cells
VCAN	Versican
WJ	Wharton's Jelly

List of figures

List of tables

Table of content

1 Introduction

1.1 Clinical relevance of the study

Damage to cartilage, bone and other connective tissues of the joint causes swelling, pain, stiffness and immobilization (loss of motion). Due to limitations in procedures for regeneration and normalization of cartilage and joint function, patients with such damages have a lifelong need for painkilling pharmaceuticals or receive an artificial joint replacement. The knowledge on joint disorders is limited due to the complex nature of immunology and pathology in these conditions. Arthritis is most common in the elderly, but also appears in the younger population, as Juvenile idiopathic arthritis (JIA) (1). The prevalence of osteoarthritis (OA) in Norway is partly uncertain, although a population survey carried out in the municipality Ullensaker in 2004 shows an overall prevalence of 12.8% (n = 3266). The numbers are rising with age and are higher among women compared to men (2). In USA, the approximate prevalence of symptomatic knee OA is 10% in men and 13% in women aging 60 years or older (3). The overall prevalence of rheumatoid arthritis (RA) from an Oslo population survey was 0.437%, concurring with the 0.5-1.0% of populations affected worldwide (1, 4).

1.2 Synovial joints

Skeleton is the framework of the human body. Joints are points of connections between two or more bones, making it possible for us to move. There are three main classes of joints (see fig. 1) (5):

- Synarthrosis (immovable)
- Amphiarthrosis (slightly movable)
- Diarthrosis/synovial joint (freely movable)

Synovial joints are comprised by articular cartilage (AC), synovial membrane (synovium), subchondral bone, ligaments and menisci (in knee joint) (6). The synovial membrane is a soft tissue derived into a continuous surface layer of cells (macrophages, fibroblasts and adipose cells) called the intima, and the underlying tissue called subintima (variety of cells, e.g. fibroblast) (7). Synovial fibroblasts produce hyaluronic acid (HA) and the glycoprotein lubricin. These are contents of the synovial fluid that allows movement by reducing adhesion within the joint surfaces. The subintima includes blood and lymphatic vessels (7-9).

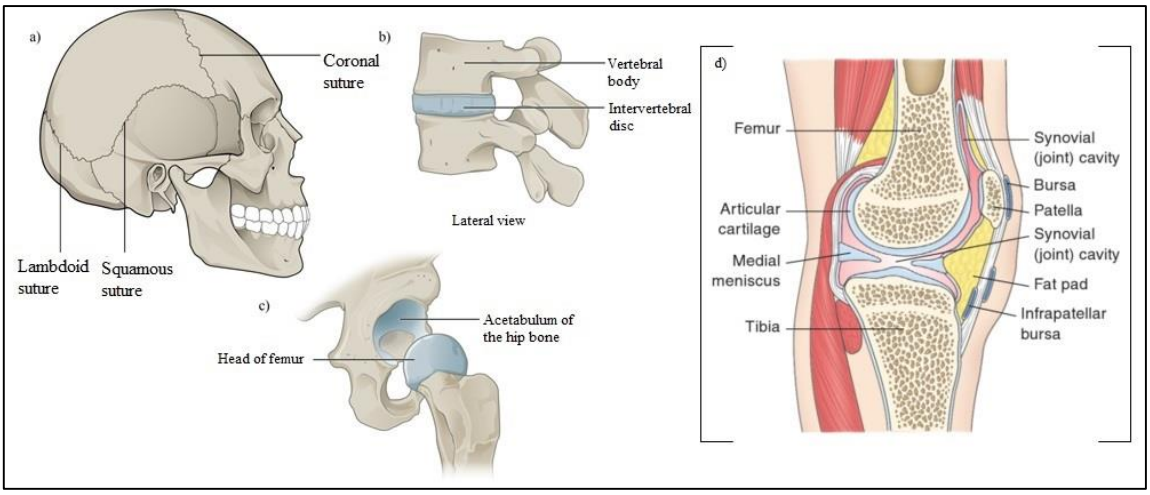

Figure 1. Types of joints. Sutures in the skull are immovable, due to their small amounts of connective tissue (synarthrosis, a). Intervertebral discs are made up of slightly movable fibrocartilage (amphiarthrosis, b). Two articulating surfaces (AC coated) in e.g. the hip, are not directly connected, making the synovial joint freely movable (diarthrosis, c). The knee hinge is another example of a synovial joint (d). Images modified and information adapted from (5, 10).

1.3 Articular Cartilage

There are three types of cartilage in the human organism (see fig.1) (11):

- Hyaline (articular) cartilage, found in e.g. synovial joints and the nose
- Fibrocartilage, found in e.g. intervertebral discs
- Elastic cartilage, found in e.g. ears

This thesis will mainly have a focus on articular cartilage (AC). The cartilage in joints works as a "shock absorber", lining the opposing bones in diarthrodial joints and providing a smooth surface for joint movement (12-14). It is composed of a solid phase of cells (chondrocytes) and macromoleculs, and a liquid phase of electrolytic water (see table 1). The tissue is avascular and aneural (lack of blood vessels and nerves) and has no lymphatic supply (8, 14). Lack of these properties makes AC a tissue with low capacity of self-repair.

Table 1. Composition of articular cartilage. Table adapted from (14).

Articular cartilage		% wet weight	% dry weight	Functions
Solid phase (ECM)*	Collagen	Type II collagen is 15 – 20% All other collagens are < 2%	50 – 75%	Contributes to tensile properties and macromolecule entrapment
	Proteoglycan	10%	20 – 30%	Contributes to compressive and flow-dependent viscoelastic properties
	Other glyco-protein, fibronectin etc.	Small amount	Small amount	Contributes to cell-ECM interactions and the stability of ECM
Solid phase (cells)	Chondrocytes	< 5 – 10% of total tissue volume		Modify ECM and maintain suitable tissue size
Fluid phase	Interstitial water and electrolytes	**60 – 80%	–	Exchanges nutrients with synovial fluid, lubricates the joint, and contributes to compressive resistance and deformation

* ECM comprise 65 – 80% of the total weight in AC

** Approximately 30% of the total water constitution in AC is found intrafibrillar (within collagen) (8)

The normal thickness of AC in a healthy knee is 1.5 – 3.0 mm (14). AC is comprised by cells, and extracellular matrix (ECM) of macromolecules, arranged differently in four horizontal layers (zones) (see fig. 2) (8). The ECM is also divided into the pericellular, interterritorial and territorial region, with chondrocytes as a baseline (14).

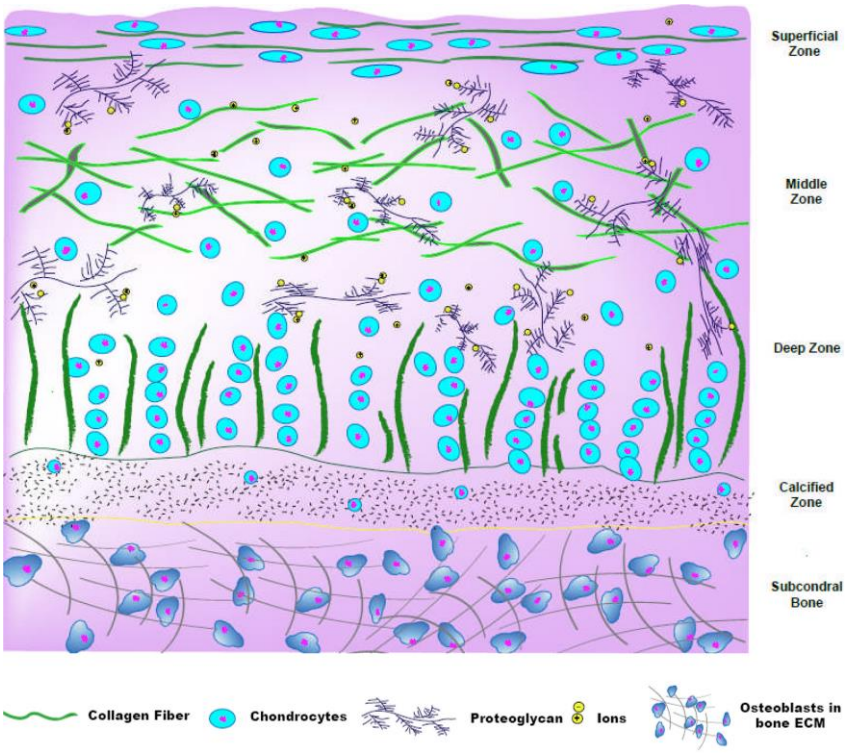

Figure 2. Schematic illustration of composition and structure in AC lining the bone. The *superficial (tangential) zone* (10-20% of the total thickness) has collagen fibers and chondrocytes tight packed in parallel to the articular surface, protecting deeper layers from shear stresses. The middle, *transitional* zone (40-60% of the total volume) consists of proteoglycans, thick collagen fibrils (organized obliquely) and has a low density of chondrocytes. It is important in resisting compressive forces. The deep *radial zone* (30% of the volume) resists compressive forces in an even greater extent, consisting of collagen fibrils (large diameters) arranged perpendicular to the articular surface. The zone has the highest content of proteoglycans and the lowest water concentration. Chondrocytes are arranged in parallel to the collagen fibers. The calcified *tide mark zone*, which being the connective layer between cartilage and bone, has a high concentration of proteoglycans yielding the highest resistance to compressive forces. The collagen fibrils are perpendicular arranged to the surface, and the chondrocytes are characteristically hypertrophic (enlarged), have a calcified ECM and express collagen X. Image adapted from (14). Information adapted from (8, 15).

1.3.1 Chondrocytes

The resident cells in AC are called chondrocytes, originating from the mesoderm of the developing embryo. They are metabolically active cells that produce and maintain the ECM of the cartilage that they essentially get trapped in (early chondrocytes are called chondroblasts) (8, 11). Therefore, they rarely form cell-to-cell contact (2-4 cells reside in lacunas within the cartilage) but are rather stimulated by growth factors, mechanical loads, piezoelectric forces and hydrostatic pressures (8, 11).

1.3.2 Extracellular Matrix (ECM)

In ECM of the AC, the protein group of **collagen** makes up the most abundant group of macromolecules. Numerous types of collagen are present, but 90-95% is represented by type II collagen, whereas the minor types represented, for instance type IX and XI, helps to form and stabilize the major type II group. A class of heavy glycosylated protein monomers (glycoproteins), **proteoglycans**, makes up the interfibrillar space of collagen. Crosslinking between collagens makes up a fibril meshwork mainly providing AC with **tensile properties**, because of interfibrillary interactions with proteoglycans (8, 14, 16). Aggrecan is the largest and most weight abundant proteoglycan in AC, and has the ability to aggregate (many

molecules of aggrecan) with a single molecule of HA (14, 16). HA is a **glycosaminoglycan (GAG)**, a group of polysaccharides with several important compounds residing in the ECM. Keratan sulfate and chondroitin sulfate are GAGs branching single aggrecan molecules. The sulfate groups (SO_3^-) in chondroitin sulfate and the carboxyl groups (COO^-) in HA make aggrecan a molecule of high negative charge. By attracting positively charged cations in the interstitial fluid of the ECM, aggrecan provides cartilage with osmotic properties, making it swell and act resistant to compressive loads (8, 14). Collagens and proteoglycans is thereby the two major load-bearing macromolecule groups present in AC (8). During loading (compression) the interstitial pressure increases, making the fluid flow out of the ECM, lubricating the joint surfaces. Load removal has the reverse effect (8, 14). This biochemical composition is showed in fig. 3 (see table 1 as well).

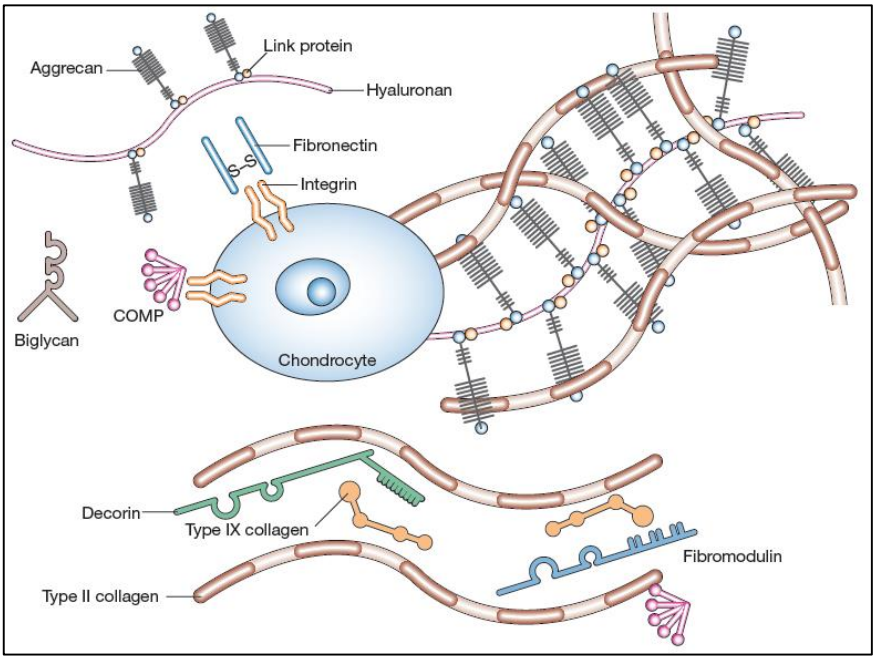

Figure 3. ECM of articular cartilage. Image adapted from (17).

1.3.3 Chondrogenesis

The process of cartilage development, *chondrogenesis*, is important in human skeletal development and skeletal repair in the adult. The process is initiated during embryo development by condensation of mesenchymal stem cells (MSCs), undergoing chondrogenic differentiation. A cartilage template (growth plate) of young cells develops while the mature cells undergo hypertrophy, making two separate regions. Vascular invasion initiates the development of bone, and the oldest chondrocytes undergo endochondral ossification (replacement with bone) separating the cartilage template from stable AC (18-20).

1.3.4 Cartilage physiology and metabolism

The lack of blood vessels in AC leaves the chondrocyte metabolism primarily anaerobic (without oxygen). Diffusion of the synovial fluid provides AC with the necessary nutrients and O_2 through the pores of the ECM. This diffusion is prevented by calcium salts (8, 20). Chondrocytes in the deep layer (calcified zone) therefore differentiate to hypertrophy and apoptosis, before undergoing endochondral ossification (15, 20-22). In adults, where cartilage and bone are fully developed, chondrocytes mainly are in a resting (inactive) state (15). Cartilage homeostasis is referring to normal metabolism of the tissue. This may be altered by chemical and mechanical factors, and proinflammatory cytokines (e.g. interleukin 1 [IL-1] and tumor necrosis factor alpha [TNF-α]). *Catabolism* in chondrocytes is linked to production of ECM degrading enzymes (proteases), augmented by stress environments such as mechanical loads, inflammation etc. Anabolism, on the other hand, refers to production of ECM macromolecules (proteoglycans, collagen) (23). Proteases involved is the *matrix metallo-proteinases* (MMPs) collagenase, gelatinase and stromelysin, the *cathepsins* (type B and D), and the enzyme family of *A Disintegrin And Metalloproteinase with Thrombospondin Motifs* (ADAMTS) (8). These seem to play a key role in regulation of tissue remodeling, breaking down collagens and aggrecan (among others) of the ECM (22, 24).

1.4 Articular cartilage disorders

Homeostasis in ECM metabolism is essential for regulation of a healthy AC, protecting chondrocytes from potentially damaging biomechanical forces. In fact, the proteoglycan turnover may take up to 25 years, and collagens have a half-life ($t_{1/2}$) from several decades up to 400 years (in healthy cartilage). ECM composition in the elderly changes because of factors like decreased hydration. Cartilage degradation is also seen in inactive patients (8). There are many groups of joint diseases (arthropathies), but OA and RA are the most common types, appearing most frequently in senior adults. Joint disorders are classically divided into two main categories; **inflammatory** (RA) and **non-inflammatory** (OA) (13). A common factor in all such diseases is the gradual and irreversible deterioration of AC (13, 14, 25).

AC defects are divided into *partial-thickness defects* and *full-thickness (osteochondral) defects*, depending on whether the damage is confined within the ECM zones or if it also punctures the underlying bone (see fig. 4 as example). Partial defects are a potential starting point for cartilage degradation, since chondrocytes alone cannot manage the restoration. In full-thickness defects, bone-marrow mesenchymal stem cells (BM-MSCs) gain access to the

lesion, being able to differentiate into chondrocytes. This is resulting in fibrocartilage production, being mechanically of inferior quality than AC. Further degradation may often result in tissue replacement by subchondral bone, inflammation, pain and disability (see fig. 5) (14).

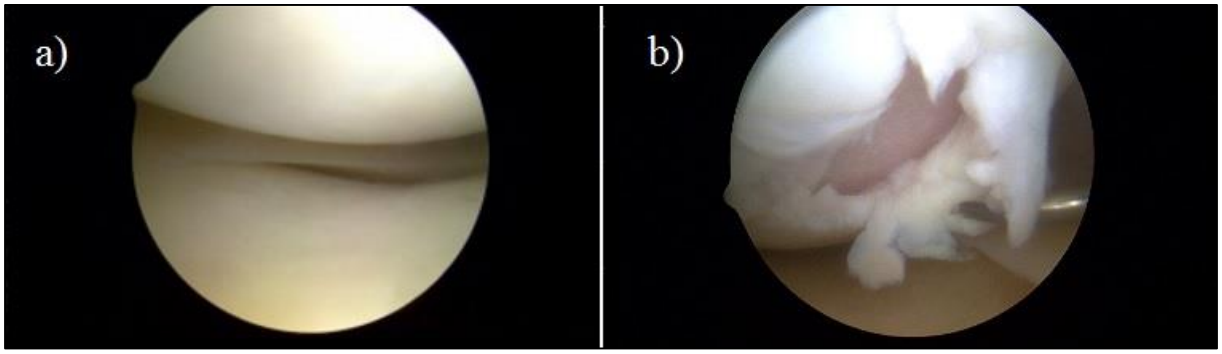

Figure 4. Cartilage lesion. Arthroscopic picture of healthy cartilage (a) and an acute cartilage lesion, where cartilage is peeling off the bone (b). Images adapted and modified from (26).

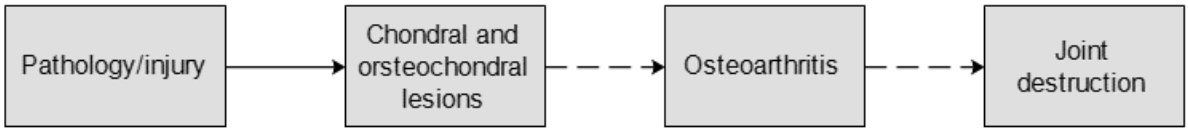

Figure 5. Pathology or injury of cartilage or osteochondral bone may lead to lesions. Over time, lesions often result in development of OA and further joint destruction. Treatment strategies differ between cartilage lesions and OA. Image made by using the software Edraw Max 7.9, 14.03.16, based on information from (27, 28).

1.5 Biological repair of cartilage injuries (focal lesions)

Several techniques for focal cartilage repair are currently applied in the clinics, aiming for AC restoration. These include direct surgery to the subchondral bone and use of tissue engineering techniques (cellular or acellular), the latter mimicking the natural environment in healthy cartilage with or without the help of scaffolds (scaffold-based or scaffold-free techniques). Table 2 shows definitions of grafting types when working with cellular transplantations. In this thesis, I will mention three of the most frequently used biological repair methods in the clinics.

Table 2. Graft (transplantation) types. Information obtained from (29).

Graft type	Definition
Autograft	Within the same individual.
Syngraft	Between genetically identical individuals.
Allograft	Between genetically different (non-identical) individuals within the same species
Xenograft	Between species (e.g. animal to human)

1.5.1 Microfracture

Microfracture is an arthroscopic marrow-stimulation procedure and probably the most widely used method in cartilage repair worldwide. It is initiated by debridement of damaged cartilage down to the subchondral bone. An angled awl is further used to penetrate the subchondral bone in several places with 3-4 mm distance, inducing bleeding. BM-MSCs, fibrin and platelets form a clot (called a "superclot") at the site of intervention (see fig. 6). The MSCs undergo chondrogenic differentiation and tissue repair (30, 31). Microfracture is considered a gold standard in its genre by the U.S. Food and Drug Administration (FDA). Although the repair in many patients is limited, only providing a delay in further degradation. This is due to the formation of less robust fibrocartilage, making the tissue more vulnerable than AC. Therefore, indications for size, depth, lesion location in the joint, patient age and BMI have to be met before carrying out the procedure (27). Microfracure is appropriate for small defects because its minimal invasiveness and short recovery time (14). A new scaffold-based microfracture technique (Autologous Matrix Induced Chondrogenesis, AMIC) has been developed, by using a collagen matrix and a glue containing TGF-β for stimulation of chondrogenesis (31).

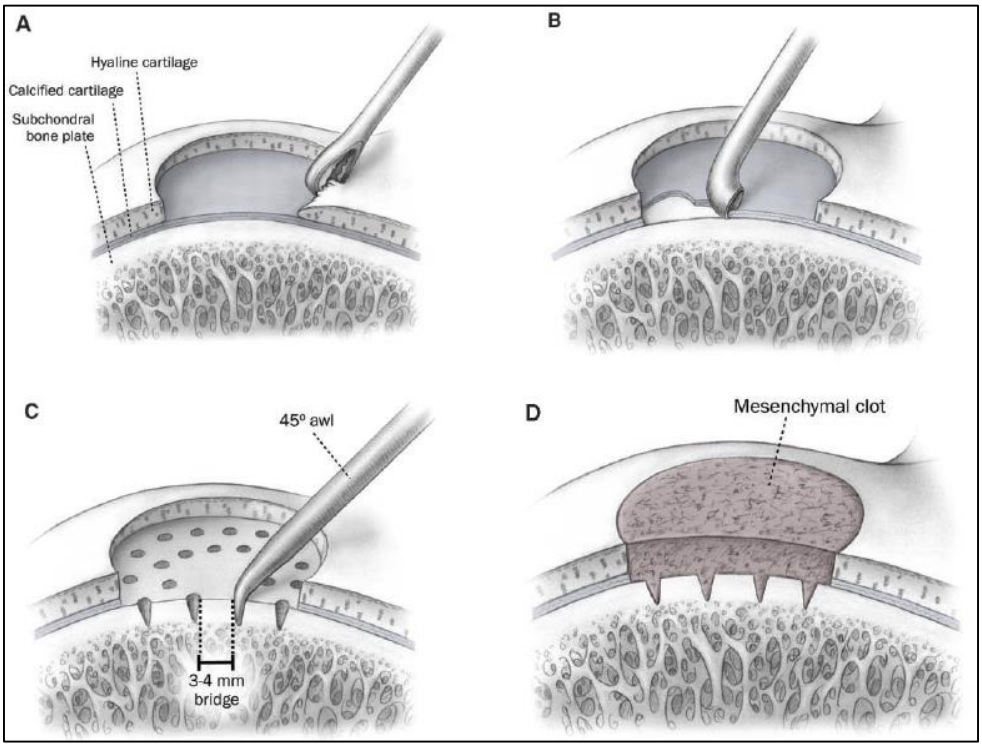

Figure 6. Microfracture. Debridement of damaged cartilage (A), followed by careful removal of the calcified cartilage (B) and penetration of the subchondral bone (C). A "superclot" will further fill the site of intervention (induced lesion) (D). Image adapted from (32).

1.5.2 Autologous chondrocyte implantation (ACI)

Autologous chondrocyte implantation, ACI (see table 2 for definition), is a technique based on a two-step procedure. Collection of a small cartilage biopsy from a non-weight-bearing region of the joint is first carried out by arthroscopy. Further *in vitro* cell expansion (one million cells/cm^2 lesion) is necessary before implantation into the patients' areas of cartilage defects (second operation). The lesion is then covered by a membrane cap, often periosteum (see fig. 7). Adverse immunologic responses (graft-versus-host disease, GvHD) are avoided by autografting (27, 30). The procedure was first carried out in 1987, and has treated cartilage lesions in over 35 000 patients since the first study in humans on this procedure in 1994 (31, 33). As a side effect, hypertrophy of the periosteal cap is often seen after repair, rising the surface friction in the joint cavity (ACI failure). Therefore, a second generation ACI using a collagen-cover (CACI), was developed. Further improvement has been made with a third generation technique, using a collagen membrane as a scaffold for seeding of chondrocytes (matrix-induced autologous chondrocyte implantation, MACI). This provides a more homogenous distribution of chondrocytes within the lesion. ACI is the most common cellular-based tissue engineering technique for the purpose of cartilage lesions (27, 30, 33). Dedifferentiation (loss of cell phenotype) is a problem when expanding cells *ex vivo*. This results in synthesis of fibrocartilage-specific collagen type I and versican (VCAN) instead of AC-specific collagen type II and aggrecan, yielding a mixture of fibrocartilage and AC, partially reduced in mechanical and osmotic properties compared to healthy AC. This is a major limitation to ACI, in addition to the necessity of two surgical procedures, being invasive and may promote donor-site morbidity (31, 33). The recovery time after ACI is relatively long (6-12 months). ACI is suitable for lesions of 1-12 cm^2 and in cases where microfracture has failed (14).

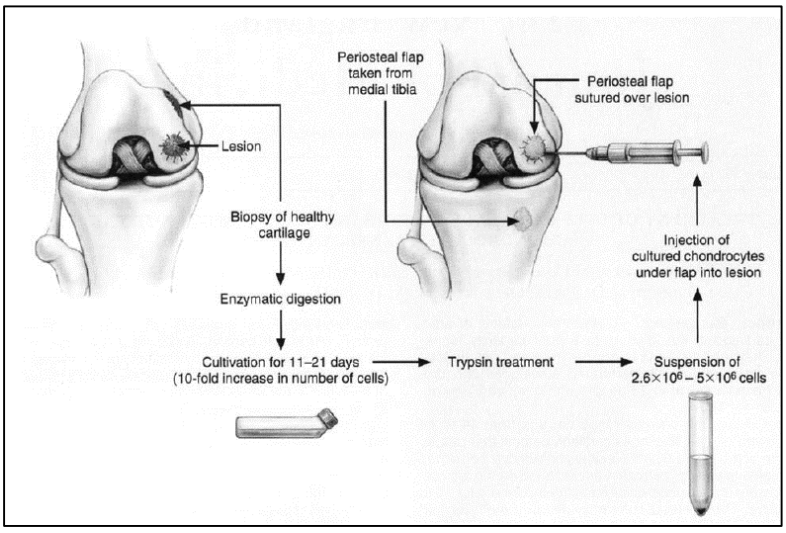

Figure 7. ACI procedure. Image adapted from (33).

1.5.3 Mosaicplasty

Basal osteochondral autografting, or mosaicplasty, is based on implanting cylinders, or plugs, of healthy osteochondral fragments into the site of cartilage lesion (see fig. 8) (14). The high level of the femoral bone (close to the knee) is often used as a source (31). Donor site morbidity, graft instability and short-term survival of the graft are problems frequently seen after these procedures, limiting its application to lesions of 1-4 cm^2. The cylinders may be of various sizes, sufficient to fill the area of lesion (14, 31). The technique is used for both chondral and osteochondral lesions, immediately giving rise to mature AC in the operated area. Because of the zonal variety in AC, the thickness may vary between the site of implantation and the donor site. Therefore, lateral integration rarely happens, enabling penetration of the subchondral layer by synovial fluid, causing cyst formation. Additionally, it is hard to produce a graft with a smooth joint-facing surface (31).

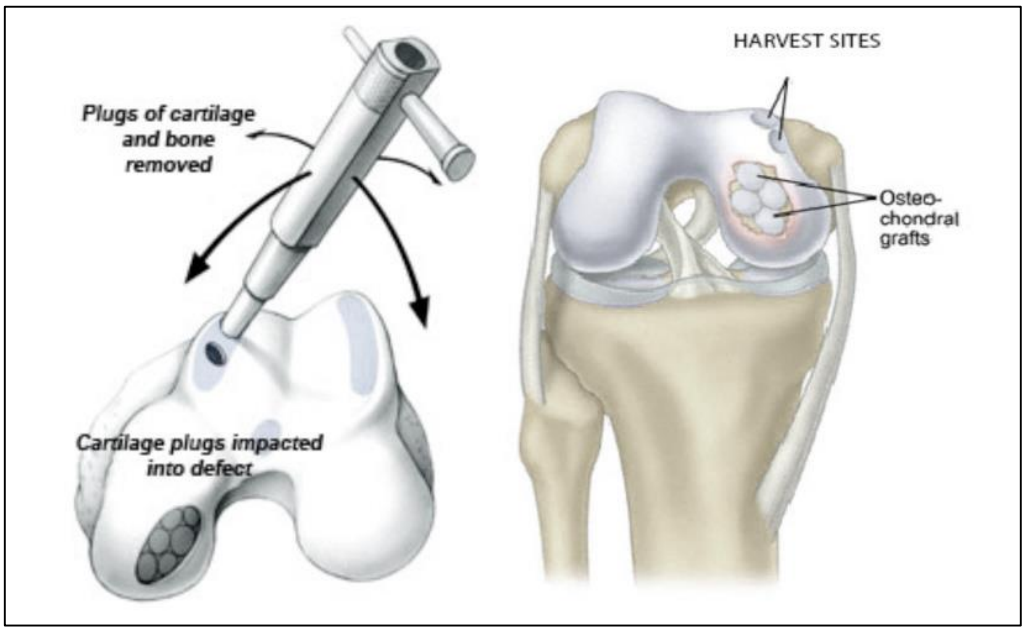

Figure 8. Mosaicplasty. Image adapted from (34)

1.6 Stem cells

The limitations associated with microfracture, ACI and mosaicplasty (invasiveness, availability and accessibility, and suboptimal repaired cartilage) have pushed researchers to search for alternative sources of cells with desired characteristics (14, 27). Stem cells are undifferentiated cells with the ability of *self-renewal* (non-differentiated) and *differentiation into multiple cell lines* (see fig. 9). Residing in tissues throughout the body, stem cells are working as buffers in situations of tissue damage, as a supply for new tissue-specific cells (e.g. blastocyst of the bone) (35). Stem cells are categorized in consideration to the number of cell lineages they can differentiate into (14).

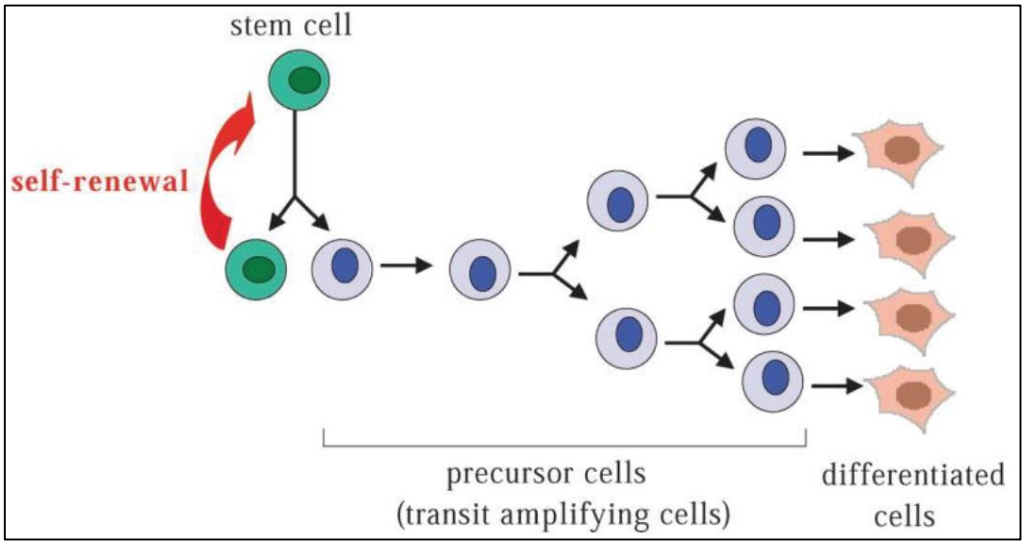

Figure 9. Self-renewal and differentiation, defining properties of a stem cell. Image adapted from (33).

1.6.1 Stem cell classifications and categories

Stem cells are mainly classified as embryonic or adult stem cells (33). In early embryonic development, cells from the three germ layers (ectoderm, endoderm and mesoderm) differentiate to form different kinds of body tissue. Cells in adult tissues therefore originate from one of these three germ layers (36). Morula cells from the intermediate cell stage between zygote (fertilized egg cell) and blastocyst (cell cluster developing into the embryo) are considered totipotent stem, able to differentiate into any kind of tissue in the body, including the placenta and umbilical cord (UC) (14, 37).

Embryonic stem cells (ESC) may differentiate to cells from any of the three germ layers and are therefore classified as *pluripotent* (14, 38, 39). Because of their huge differentiation

potential, they are considered the most promising cells for regenerative medicine. However, use of ESCs is associated with ethical concerns, and hence they are not widely used. Alternatively, induced Pluripotent Stem Cells (iPSCs), sharing many properties of the ECS, may be produced in the laboratory (39). The tumorigenic potential (teratoma formation) of such embryonic cells (ESCs and iPSCs), when transplanted *in vivo*, rises further concerns (39, 40). Adult stem cells (ASCs) are stem cells with the ability to differentiate into multiple closely-related cell types only, and are by this categorized as *multipotent* (33). MSCs is another group of multipotent stem cells, described more detailed later (14). Examples of all stem cell categories is shown in fig. 10.

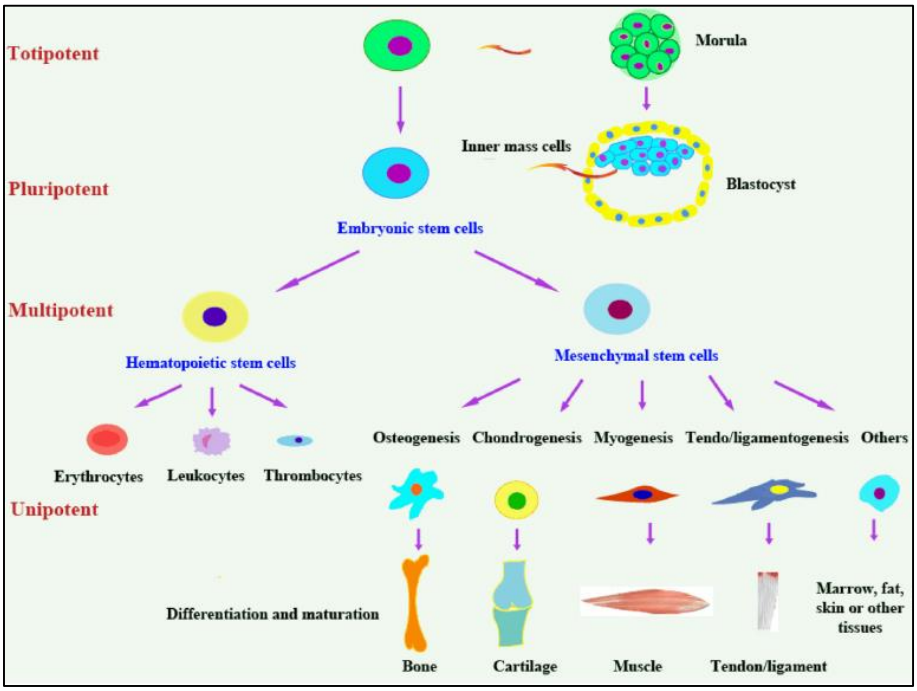

Figure 10. Totipotent, pluripotent, multipotent and unipotent stem cells. Image adapted from (14).

1.6.2 Adult stem cells (ASCs)

Stem cells present in most tissues of the adult human body are called adult stem cells (ASCs). Their main role is to maintain tissue homeostasis by replacing cells undergoing apoptosis due to normal tissue turnover or injury (working as cell reservoir). Self-renewal and differentiation is possible due to their response to signals from other stem cells (in the "stem cell pool") and other specialized cells in the tissues. ASCs have a more restricted differentiation potential than ESCs, being more correspondent to the tissue they originate from (multipotency) (33).

1.6.3 Mesenchymal stem cells (MSCs)

MSCs exist in connective tissues throughout the body and are commonly obtained from bone marrow (BM), adipose tissue (AT), umbilical cord (UC), and others. Harvesting of MSCs often causes undesired invasiveness and pain (e.g. BM-MSCs), dependent on the tissue source (40, 41). Because MSCs are multipotent and non-tumorigenic, they represent an attractive alternative to ESCs and iPSCs. Unfortunately, MSCs have a lower differentiation potential and lower frequency of tissue repair compared to ESCs (40). MSCs were thought to be originated from the mesoderm, but they also have the ability to differentiate into certain cell strains coming from the endoderm and ectoderm. Their ability to keep their multipotency and being non-tumorigenic are making them interesting for regenerative medicine, and hence an interesting source for AC (39, 40, 42).

1.6.3.1 Hoffa's Fat Pad Derived Mesenchymal Stem Cells (HFP-MSCs)

AT is easy accessible (can be harvested subcutaneously) and is abundant in the body, being a potentially good source of MSCs since they also seem to share some characteristics with the widely used BM-MSCs. Compared to BM- and cartilage derived MSCs, they possess high capacity of proliferation (43, 44). The Infrapatellar Fat Pad (IFP) or Hoffa's Fat Pad (HFP) is an adipose part of the synovium in knee joints (see fig. 1). Its physiological function is uncertain, although it might play a role for distribution of synovial fluid by enlarging the synovial area. Since collecting such tissues from healthy patients is restricted, HFP is often collected from patients undergoing full joint replacement (e.g. in OA) (43). HFP- and synovial membrane (SM) derived MSCs (HFP- and SM-MSCs) have been shown to hold high chondrogenic potential compared to BM- and muscle derived MSCs (45). HFP-MSCs are similar to AT-MSCs in surface marker expressions, and they are similar to BM-MSCs in proliferation and differentiation towards chondrogenic, adipogenic and osteogenic lineages

(43, 46). Differentiated HFP-MSCs is a good source for autologous transplantation in patents with OA (47).

1.6.3.2 Umbilical Cord Derived Mesenchymal Stem Cells (UC-MSCs)

UC has earlier been considered as biological waste, but today it is seen as a potential non-invasive and painless source of MSCs (38, 48). It consists of two arteries and a vein, surrounded by a connective tissue called Wharton's jelly, WJ (see fig. 11). MSCs can be isolated from different regions such as WJ, cord lining, the perivascular region (region surrounding the blood vessels), or from the whole cord (mixed cord, MC) (38). UC-MSCs have been shown to have a differentiation capability of cells from mesoderm (adipocytes, osteocytes and cartilage), ectoderm (neurons, astrocytes and glial cells) and endoderm (hepatocytes and insulin-producing islet cells), and have immunomodulatory and anticancer effects (in certain types of cancer). The use of UC as a source for MSCs yields a low risk of infection (38, 48). MC derived MSCs (MC-MSCs) have previously shown properties for chondrogenic and adipogenic differentiation, compared to cells isolated from any of the separate compartments (49). However, a recent study within our research group concluded poor chondrogenic potential of MC-MSCs (41). MC-MSCs are highly proliferative and can be frozen with an acceptable number of viable cells after thawing. Additionally, they fulfill the requirements for use in stem cell banking, being potential in use for this purpose, of which umbilical cord blood commonly is applied. The differentiation capacity of UC-MSCs also seems to be better than UC blood cells. The cord cannot be frozen, as it should be as fresh as possible before stem cell isolation (38, 49).

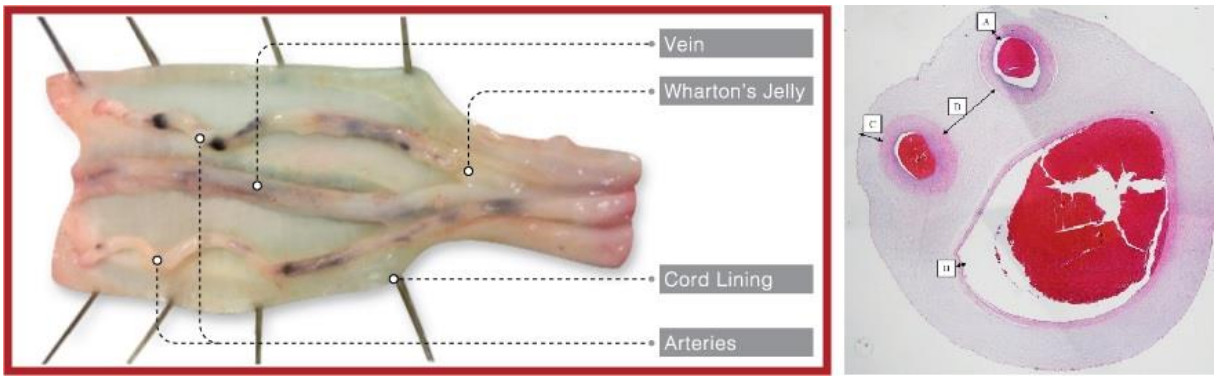

Figure 11. Different regions of a human umbilical cord. Image to the left shows a dissected cord. Image to the right shows to small arteries and one big vein in an umbilical cord cross-section. Left image adapted from (50). Right image adapted from (51).

1.6.4 Multilineage-differentiating stress-enduring (MUSE) cells

In 2010, Kuroda et al. presented the discovery and isolation of a novel multipotent cell **residing in MSC populations** of many different adult tissues. However, they differ from the normal bulk of MSCs by being positive for the **pluripotency** marker Stage-Specific Embryonic Antigen-3 (SSEA-3). Single cells are able to **endure stress conditions**, undergo **self-renewal** and differentiate into cells of **mesodermal**, **ectodermal** and **endodermal** lineages (triploblastic differentiation) both *in vivo* and *in vitro*. Therefore, they were given the name *multilineage-differentiating stress-enduring cells (MUSE-cells)* (52, 53). Concomitant to being SSEA-3$^+$, they are positive for the mesenchymal stem cell markers CD105, CD90 and CD29 (54). They also show functional characteristics similar to cells of both multipotency and pluripotency. Like fibroblasts, they **attach to surfaces** when they are in adherent state (culture or connective tissues), and in suspensions (e.g. blood), they show the similar behavior to ESCs as they are able to **form cell clusters** from single cells (40). When injected into immunodeficient mice, they home towards damaged tissues where they differentiate, and seem to play an important role in **tissue repair** (see fig. 13)(53). Sorting of SSEA-3$^+$ MUSE-cells from a population of MSCs makes it possible to distinguish between *MUSE*- and *non-MUSE cells* (the latter being SSEA-3$^-$ cells). In one study, both MUSE- and non-MUSE cells were induced towards pluripotency (generation of iPSCs). Interestingly, the MUSE-cells seemed to generate 30 times more iPSCs compared to those generated from non-MUSE dermal fibroblasts, suggesting that MUSE-cells are a primary source of iPSCs. MUSE-cells and non-MUSE cells may therefore play different roles within the body (see fig. 12) (40, 54, 55).

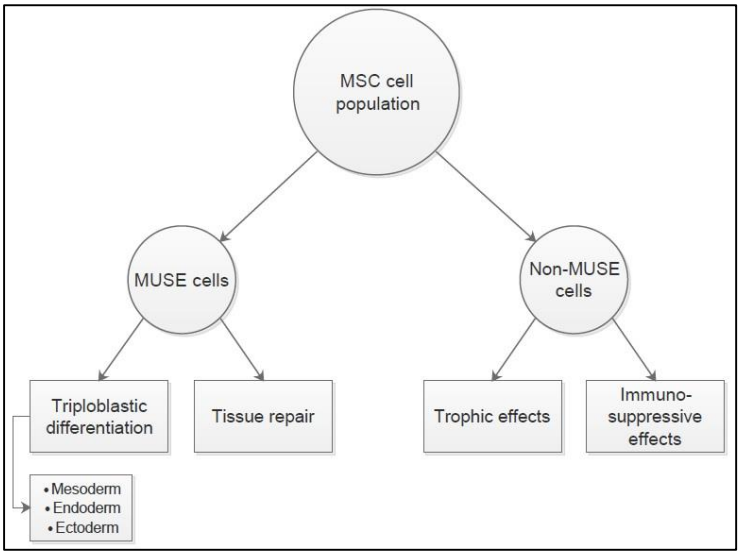

Figure 12. Suggested properties of MUSE cells and Non-MUSE cells. It has been suggested that MUSE-cells differ from non-MUSE cells in properties of activity. MSCs are for instance able to modulate immunologic reactions through production of humoral factors (trophic factors). MUSE-cells may hold the ability to differentiate into cells from the three germ layers (triploblastic differentiation) and thus working as a trouble-shooter in tissue damage (referred to as "regenerative homeostasis"), but seem to differentiate into cells of the mesodermal lineage most frequently. Image made by using the software Edraw Max 7.9, 29.10.15, based on information from (40).

The concerns of teratoma formation associated to the use of ESCs and iPSCs does not seem to apply for MUSE-cells. This characteristic was checked experimentally: *In vitro* prepared MUSE-cell derived clusters (M-clusters), from single-cell cluster formation assay, and populations from MUSE Enriched Cell cultures (MEC), obtained by long-term trypsin incubation (LTT), were injected into the testes of immunodeficient mice. In conclusions, MUSE-cells didn't seem to form teratomas (**non-tumorigenic**) in the test models, even after 6 months. This may be a reflection of their **low telomerase activity**, an indication for limited replication potential. These characteristics make MUSE-cells an interesting source for regenerative medicine (52, 54, 55). As an example, it has lately been demonstrated that they are able to undergo differentiation into melanocytes *in vitro*, induced by cytokines and growth factors in 3D culture. Transplantation onto immunodeficient mice showed positive results for both epidermal integration and melanin production *in vivo* (56).

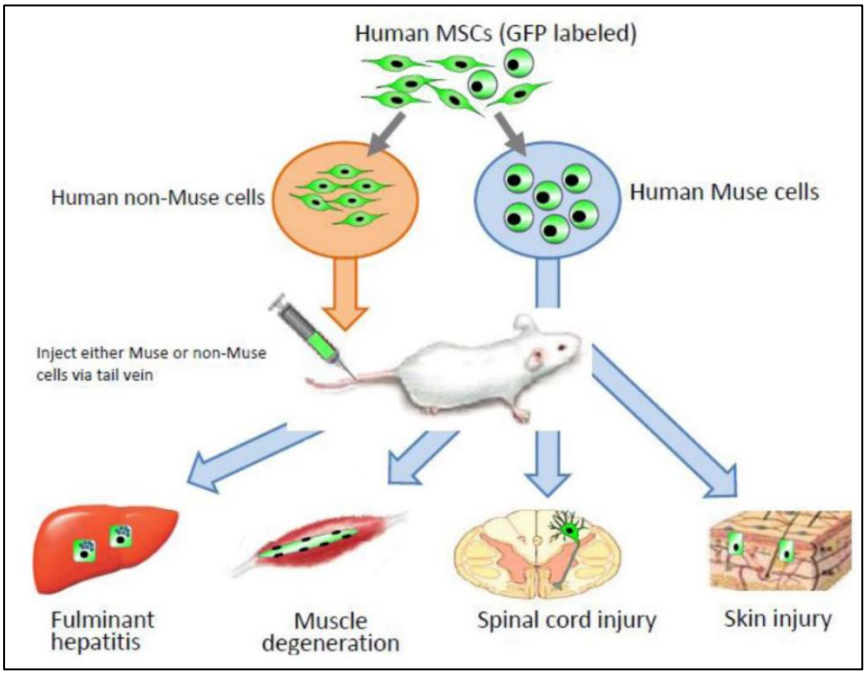

Figure 13. Tissue repair by MUSE-cells. Picture showing homing and differentiation capacity of MUSE cells after injection in the peripheral blood stream of immunodeficient mice (*in vivo*). The cells integrate in damaged tissues and spontaneously differentiate into tissue-specific cells, due to the microenvironment. This has been demonstrated in fulminant hepatitis, muscle degeneration, spinal cord injury and skin injury in these animal models. Image adapted from (53).

MUSE cells have so far been obtained from sources like BM, AT, dermis and commercially available fibroblasts. Among these, BM-derived MUSE cells seem to be of a higher pluripotency (40). MUSE-cells in M-clusters proliferate for a certain number of days, until stagnation. Proliferation is continued when they are transferred to adherent culture, using approximately 1.3 days per cell division (52, 53). MUSE-cells can be distinguished from MSCs and collected by the following techniques, where the FACS method is most frequently demonstrated:

- Fluorescence-activated cell sorting (FACS, flow cytometry)

  CD105/SSEA-3 double-positive sorting directly from tissues (e.g. bone marrow aspirates) or single-positive for SSEA-3 when sorted from MSC cultures. LTT treatment is a method yielding a so-called MUSE-Enriched Cell (MEC) population, and may enrich the culture with MUSE-cells (52). Single-cell suspension culture is further used to prove that the cells sorted are MUSE-cells (see fig. 14)(54).

- Severe cellular stress treatment (SCST)

  Long time incubation of tissue with collagenase in low temperature, serum deprivation and hypoxia and a further incubation procedure, yielding very pure populations of MUSE-cells. This method has been demonstrated for AT, without need for any FACS procedure (57).

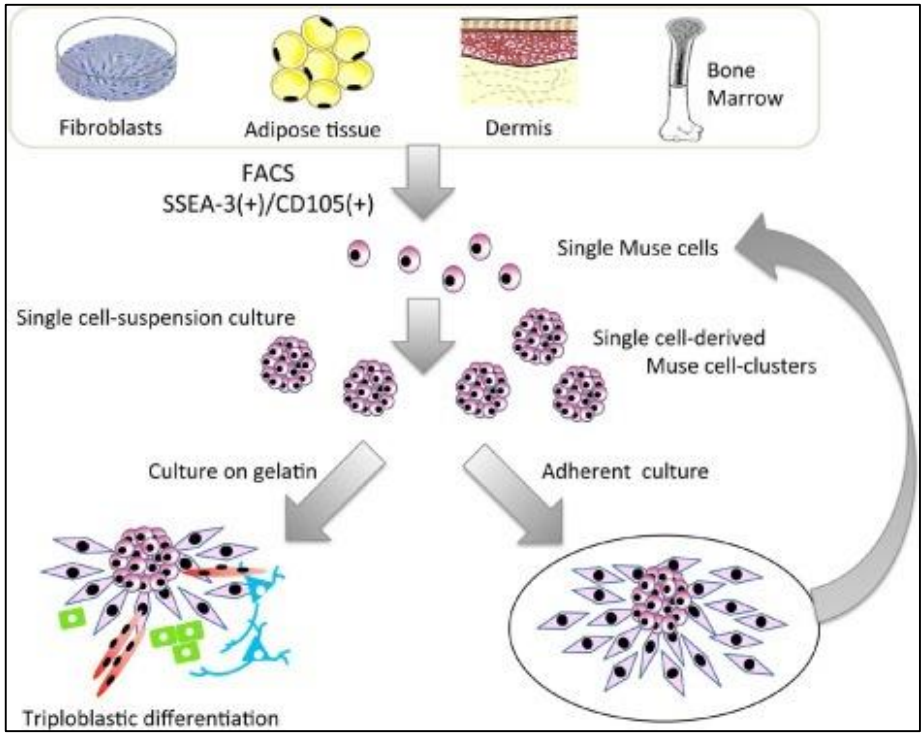

Figure 14. Isolation of MUSE cells and M-cluster formation. Image adapted from (40).

2 Aims of the study

MSCs from different tissues have different chondrogenic potential. MSCs harvested from Hoffa's fat pad (HFPSCs) display good chondrogenic potential, but its collection is invasive. Umbilical cords (UCs) are more accessible, very abundant and its collection is not associated with co-morbidities, however, UC-derived MSCs show bad chondrogenic potential *in vitro*. Importantly, it has recently been described the existence of a subclass of MSC within the main population of MSCs called MUSE-cells, associated with higher differentiation potential and repair capacity than the whole bulk of MSCs.

Our hypothesis is that MUSE-cells isolated from primary cultures of MSCs, display increased chondrogenic potential than the whole bulk of MSCs *in vitro* and thus they would be more suited for transplantation strategies.

Based on this hypothesis, the specific aims proposed for this thesis are:

1. To establish protocols for isolation and characterization of MSCs from HFPs and UCs
2. To establish protocols for isolation of MUSE-cells from HFP-MSC and UC-MSC cultures
3. To characterize phenotypically and functionally the isolated MUSE-cells
4. To explore the chondrogenic capacity of isolated MUSE cells

3 Materials and methods

3.1 Materials and Reagents

Table 3. List of materials and reagents used in the project

Material/Reagent	Catalog #	Producer
24-well ultra-low attachment surface plate	*734-1584*	Corning lifeScience, USA
96-conical bottom well plates	*249935*	ThermoScientific, Denmark
Anti-Stage-Specific Embryonic Antigen-3 Antibody (SSEA-3 Antibody)	*MAB4303-I*	Millipore, USA
Anti-Stage-Specific Embryonic Antigen-4 Antibody (SSEA-4 Antibody)	*MAB4304*	Millipore, USA
Agarose	*V3121*	Promega corporation, USA
Basic fibroblast growth factor (bFGF)	*100-18C*	Peprotech, UK
BD stemflow hMSC analysis kit	*562245*	BD Biosciences, USA
Bovine Serum Albumin (BSA)	*A2058*	Sigma-Aldrich, Germany
Cell strainer, 70 µm	*431751*	Corning lifeScience, USA
Collagenase XI	*C9407*	Sigma-Aldrich, Germany
Dexamethasone (DEX)	*364897*	Galen, Germany
Dimethyl Sulfoxide (DMSO)	*WAK-DMS-10*	Wak-chemie Medical GMBH, Germany
Dulbecco's modified eagle's medium (DMEM)	*D5796*	Sigma-Aldrich, Germany
Dulbecco's phosphate buffered saline (PBS)	*D8537*	Sigma-Aldrich, Germany
Ethylenediaminetetraacetic acid (EDTA) disodium salt dihydrate	*E5134-500G*	Sigma-Aldrich, Germany
Enzyme-free dissociation solution	*S-014-B*	Millipore, USA
Ethanol (EtOH)	*32221*	Sigma-Aldrich, Germany
Fetal Bovine Serum (FBS)	*50615*	Millipore, USA
Fluorescein (FITC)-conjugated AffiniPure Goat Anti-Rat IgM	*112-095-075*	Jackson ImmunoResearch, USA

Materials list continued:

Goat anti-Mouse IgG (H+L) Secondary Antibody, Alexa Fluor ® 546 conjugate	*A-11003*	ThermoScientific, Denmark
Human Bone Morphogenetic Protein-2 (BMP-2)	*120-02C*	Perprotech, UK
Human serum albumin (HSA)	*054376*	Octapharma, Switzerland
Insuline-Transferrin-Selenium (ITS)	*392-2505*	Peprotech, UK
L-Ascorbic acid	*103033E*	Analar BDH laboratory, UK
Methylcellulose (MC)	*M0512*	Sigma-Aldrich, Germany
Minimum Essential Medium Eagle, alpha modification(α-MEM)	*M4526*	Sigma-Aldrich, Germany
Non-vented culture flasks, 25 cm^2	*156340*	ThermoScientific, Denmark
Nunc cell culture flask, 175 cm^2	*159910*	ThermoScientific, Denmark
Nunc cell culture flask, 75 cm^2	*156499*	ThermoScientific, Denmark
NTERA-2 cl. D1 cells	*ATCC CLR-1973*	LGC Standards, USA
Paraformaldehyde	*158127*	Sigma-Aldrich, Germany
Penicillin and Streptomycin (P/S)	*P4333*	Sigma-Aldrich, Germany
Poly (2-hydroxyethyl methacrylate), Poly-HEMA	*P3932*	Sigma-Aldrich, Germany
TC Plate 24 Well, Suspension, F	*3922500*	Sarstedt, Germany
Transforming growth factor β1 (TGF-β1)	*100-21C*	Preprotech, UK
Transforming growth factor β3 (TGF-β3)	*100-36F*	Preprotech, UK
Trypan Blue stain solution	*17-942E*	Lonza Group, Switzerland
Trypsin-EDTA 0.25% solution	*T4049*	Sigma-Aldrich, Germany

3.1.1 Basal cell growth medium

Today, several combinations of cell growth medium are available. Compared to the original Basal Medium Eagle (BME), these consist of modified amounts of amino acids, glucose and other nutrients promoting cell growth. In our study we used Dulbecco's Modified Eagle Medium (DMEM) and Minimum Essential Medium Eagle Alpha Modification (α-MEM) as basal medium. DMEM supplies cells with a sufficient amount of carbohydrates, and are used to control cell growth and differentiation (58). α-MEM meets the specific nutrition demands of certain cells (e.g. fibroblasts), including a high concentration of amino acids (59) important in protein synthesis and energy production (60). Phosphate Buffered Saline (PBS) is a water-based salt solution containing sodium phosphate, sodium chloride and (sometimes) potassium chloride and potassium phosphate. The basic solution is isotonic and tolerated by most cell types (61). In this study, PBS was used for flushing of equipment and dilution of suspensions. We've noticed that MC-MSCs are growing better in α-MEM compared to DMEM.

3.1.2 Supplementations and serum enrichment of basal medium

Penicillin and streptomycin (P/S) are effective in action against gram-positive and gram-negative bacteria and prevent bacterial contamination. Ascorbic acid (AA) act as a reducing agent and stimulate MSC proliferation without loss of phenotype and differentiation potency. P/S and AA were therefore added to newly opened flasks of basal medium (both DMEM and α-MEM). Glutamine is an important amino acid in cell cultures, which usually is a part of normal basal medium. Problematically, spontaneous degradation of L-glutamine yields ammonia as a toxic by-product. Therefore, a stabilized solution of L-glutamine (Glutamax ®) was added to newly opened flasks of α-MEM.

1 ml of P/S, AA and Glutamax were all added per every 100 ml of basal medium.

This basal medium was supplemented with Fetal Bovine Serum (FBS), rich in growth factors, nutrients and proteins (and stripped for antibodies) (62), before cell culture application. Medium with 20% FBS (medium + 20% FBS) was prepared for use in adherent cell cultures directly after isolation from tissue. A mixture of 90% medium and 10% FBS (medium + 10% FBS) was further used when old medium was replaced, every 3-4 days of culturing.

Based on their morphology, it is common to differ between epithelial-, lymphoblast- and fibroblast-like cells. Fibroblast-like cells are connective tissue cells elongated in shape and growing in attachment to a substrate (63). Cells isolated from connective tissues, like AC chondrocytes, are already fibroblast-like cells. Stem cells are, on the other hand, tissue-unspecific. We therefore had to stimulate them into fibroblast-like cells by supplementing the

serum-based medium with basic fibroblast-like growth factor, bFGF (50 µl bFGF to 50 ml of serum-based medium).

3.1.2.1 Preparation of freezing medium

Freezing medium consisting of 70% basal medium, 20% FBS and 10% dimethyl sulfoxide (DMSO) was prepared before cryopreservation (freezing) of cells in liquid nitrogen. DMSO lowers the cooling rate and reduces the freezing point, lowering the risk of ice crystal formation which may be lethal for the cells. DMSO is therefore a cryoprotective agent (64).

3.1.2.2 Preparation of Chondrogenic medium

Stem cells transferred from monolayer to pellets or aggregates attach to each other and form tissue-like structures. Cell spreading is avoided by conducting incubations in low binding plate. This initiates spheroid-formation (ball of cells). At this point it's important to add medium enriched with growth factors for stimulation of chondrogenic differentiation. Basal medium was supplemented with dexamethasone (DEX), insulin-transferrin-selenium (ITS), transforming growth factor beta (TGF-β1 or TGF-β3) and bone morphogenetic protein 2 (BMP-2), a mixture recommended in several publications (see table 4) (18).

Table 4. Concentrations and dilutions from stock solution to medium solution. Eppendorf tubes were kept in the freezer (-20 °C) until use. Before application, they were thawed by hand and briefly centrifuged. The research group had previously found the following cocktail of growth factors most suitable for chondrogenic differentiation of MSCs, and TGF-β_3 (not β_1) was used in this project (41).

	Stock	**To cells**	**Dilution from stock (Eppendorf)**	**In 10 ml medium**
TGF-β1/3	10 µg/ml	10 ng/ml	1:1000	10 µl
BMP-2	10 µg/ml	100 ng/ml	1:1000	10 µl
bFGF	25 µg/ml	25 ng/ml	1:1000	50 µl
DEX	4 mg/ml	1 µg/ml	1:4000	2,5 µl
ITS mix	5 mg/ml insulin	5 ng/ml	1:1000	10 µl of mix
	5 mg/ml transferrin	5 ng/ml	1:1000	
	5 mg/ml selenum	5 ng/ml	1:1000	

3.2 Human material

In our study we used human UCs and the adipose tissue of HFPs (referred to as infrapatellar fat pads or sometimes subintima) as sources for MSCs. For UCs, a section of the entire cord (mixed cord, MC) was used. HFPs were obtained from patients undergoing full joint replacement due to advanced OA. UCs were delivered from the maternity ward at the University hospital of North Norway (UNN) directly after births. Both of these specimen types were delivered from UNN under donors' informed consent, even though UC is considered medical waste. An overview of methods used is shown in fig. 19.

3.3 Primary cell cultures

Tissue cells established for first time in culture dishes are referred as primary cell cultures. Cells in adherent culture (monolayer) are growing next to each other with approximately one cell thickness in height. The term *confluency* defines the density of adherent cells in a culture flask (in percentage). *Dissociation* of cells adherent culture is the method of passaging them to a new adherent culture, a cryotube or similar (increase in passage number). The confluence is desired to be approximately 70-80% prior to each passage. Higher confluency often makes it harder to get all the adherent cells detached.

3.3.1 Enzymatic digestion of Hoffa's Fat Pad (HFP)

HFP has a characteristic yellow color while SM is white or light red, being delivered in one piece. These were initially separated (carefully) and placed in different Petri dishes (see fig. 15) before specific isolation of MSCs from HFP (HFP-MSCs). The HFP was mechanically minced into small pieces (2 mm^3) before planting in a T-25 non-vented culture flask. 10 ml collagenase type XI (1.25 mg/ml) was added to the flask, which was placed on a shaker for 1 hour and 30 minutes at 37 °C. The suspension (cells, remaining tissue and Collagenase) was transferred to a tube and centrifuged at 800 xg for 10 minutes to separate the cells and the remaining tissue from the Collagenase. Collagenase was removed and the remaining pellet of cells and tissue was resuspended and planted in a 75 cm^2 vented culture flask in a sufficient amount of basal growth medium + 20% FBS.

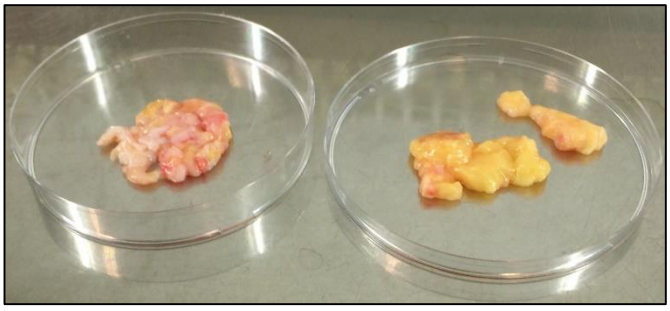

Figure 15. Synovial tissues. Hoffa's fat pad (right) separated from the synovial membrane (left).

3.3.2 Enzymatic digestion from Human Umbilical Cords (UC)

MC cultures were named based on the number of previously delivered cords, e.g. MC13 (mixed cord delivery number 13). After washing and rinsing of whole cords, they were cut approximately 2 cm in length (see fig. 16). Following was the standard PBS washing (twice), EtOH immersion (30 seconds) and PBS rinsing to eliminate bacteria contaminating the cords from births. Each of the MC cutoffs were mechanically minced into pieces of 1-1.15 cm^3. 10 ml collagenase type XI (1.25 mg/ml) was applied to the tissue in a T-25 non-vented flask, placed on a shaker for 1 hour and 30 minutes at 37 °C. Further centrifugation of the suspension at 800 xg for 10 minutes yielded a pellet (cells and tissue), which was resuspended in medium + 20% FBS and planted in a 75 cm^2 cell culture flask. Schematically illustration of this procedure (called *explant culture*) is to find in Appendix A.

Figure 16. Umbilical cord section (cutoff).

3.3.3 Cell cultures and expansion in monolayers

Cells in adherent culture are limited to expand in the area they are given, the area in cell culture flasks. For cell expansion, passaging to new flasks was done upon 70-80% confluence. Trypsin and the necessary medium were prepared for use in an oven at 37°C.

The old medium was removed from the flask, before flushing it twice with sterile PBS or basal medium (not directly applied to the cell growing surface). Dissociation of adherent cells from the flask was carried out by adding 4-6 ml of Enzyme free solution® directly to the cell growing surface and further incubation at 37°C for at least 10 minutes. Microscope was used to control cell detachment, promoted by simultaneously tapping on the flask. 1 ml 0.25% trypsin-EDTA solution was added to the flask, followed by 3 minutes of waiting so that the trypsin could work. Trypsin is a digestive enzyme which degrades protein, used for definite cell-detachment from the flask and from other cells. Inactivation of trypsin was carried out by adding 5-6 ml of basal medium (inactivation by dilution). The solution (cells, Enzyme free solution®, medium and trypsin) was transferred to a 15 ml tube and centrifugated at 800 xg for 5 minutes. The medium was removed leaving a pellet of cells in the bottom of the tube.

Fresh flasks were filled with a sufficient amount of medium + 10% FBS. The pellet was resuspended in 1 ml medium + 10% FBS per new flask we were splitting into. The flasks were set for incubation at 37°C in high or low O_2 (hyper- or hypoxia) for cell attachment. Freezing medium was used to resuspend the pellet when we were freezing cells in cryovials (1 ml cell suspension per vial).

3.3.4 Culturing of NTERA-2 cells

The embryonic carcinoma (EC) cell line, NTERA-2 clone D1 (T2/D1), is a pluripotent cell line originally derived from human lungs in the 1980s, due to metastasis from the testicles. Cells used for culturing in this project was ordered from LGC Standards, USA. Similar to ESCs and MUSE-cells, they are positive for the glycosphingolipid cell surface marker Stage-specific Embryonic Antigen-3 (SSEA-3) (65). ECs are easier to obtain and has no ethical concerns for use, compared to ESCs. Additionally, they would be able to make single-cell spheroids, like MUSE-cells. Because of this, we wanted to use these cells as a positive control in the phenotypic characterization and single-cell formation assay of our MUSE-cells. The cells were cultured under the same condition as other cells (adherent culture with α-MEM + 10% FBS in high O_2), but differed in proliferation rate, due to their uncontrolled cell division. Medium was changed every 3-4 days or more often if the number of dead cells in the medium seemed high. This continued until a sufficient amount of cells (confluency) in a T-25 flask, ready to run characterization by flow cytometry.

3.4 Phenotypic characterizations and sorting of cells by flow cytometry: principles

For characterization of MSCs phenotype and isolation of MUSE-cells, the BD FACSAria III (fluidic cell sorter machine) was used. This method allows discrimination of cells within a population according to their physical and biochemical characteristics. Cell sample preparations was carried out prior to the analysis, based on cell detachment, cell count, PBS flushing and immunostaining with primary and secondary antibodies. The primary antibody is specific for a certain cell surface marker (cluster of differentiation, CD), presumed presented by the cells. The secondary antibody is conjugated with a fluorescent dye, and attaches to the primary antibody. After adding each of these antibodies, incubation on ice with regular mixing was following (varying expenditure of time according to protocol-type). Ice is preventing aggregate formation (66). When the cell solution is presented to the machine, it's being processed for presentation of single cells aligned one by one to a laser beam. Lights are then scattered forward and sideways, being captured by detectors and converted to data on a

computer. Antibody-linked fluorophores (e.g. fluorescein isothiocyanate, FITC) are used to detect certain surface markers, as they are excited by the laser. Emission of light within certain wavelengths is then detected by the computer to determine the proportion of the sample, which is presented in a histogram (dot plot). This principle is presented in fig. 17.

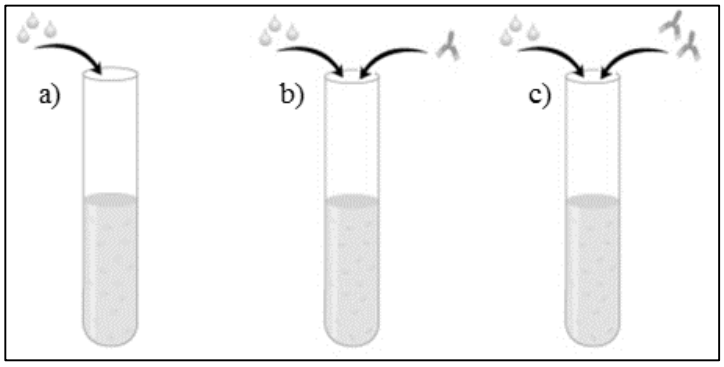

Figure 17. Principles of sample preparation for flow cytometry. A tube with only cells (a) is prepared to detect autofluorescence, since this might be present in the specimen. Another tube holding cells and secondary antibodies with a fluorescent dye (does not attach to the cell surface) is prepared (b). Tube a) and b) are both negative control, used to distinguish light emitted by the cells themselves from light emitted by the secondary antibody. These are compared to a tube with positive control (c), holding cells, primary and secondary antibodies. The primary antibody attaches to its corresponding cell surface marker and the secondary antibody attaches to the primary antibody. The secondary antibody absorbs and emits light in a wavelength (nm) made known by the manufacturer. Image adapted and modified from (67).

3.4.1.1 Buffer preparation for flow cytometry

The flow cytometry protocol we were using for phenotypical characterization of MSCs was recommending us to wash cells with stain buffer (FBS). Due to economic concerns, we made a similar washing buffer consisting of 98% sterile PBS and 2% FBS, which later will be referred to as stain buffer. The buffer was stored in the fridge (2-4°C) until use.

For sorting of MUSE-cells by flow cytometry, a washing buffer for sample preparations was made. This was called a fluorescence activated cell sorting (FACS) buffer, and was used similar to the stain buffer used in MSC characterization. The FACS buffer was consisting of 10% BSA-solution, 2% EDTA-solution (both of these were dry powder dissolved in PBS) and 88% sterile PBS. BSA was added to support the cells with protein (68). 30 ml FACS buffer was sufficient for each cell culture used. A 10 ml buffer consisting of 90% sterile PBS and 10% HSA was also prepared for use when we followed the MUSE-protocol (PBS+HSA buffer) Incubation with this buffer would reduce unspecific binding of the antibodies.

3.4.1.2 Phenotypical characterization of MSCs

Mesenchymal stem cells (MSCs) are characteristically positive for the surface markers CD90, CD73 and CD105, and negative for markers like CD34, CD45. They *may* also express CD44, CD29, CD146 and CD166, to mention a few (69). Therefore, we chose to use antibodies corresponding to CD90, CD44, CD105, CD73, CD106, CD146 and CD166 for phenotypical characterization of MSCs (definitions in Appendix B). The markers CD45, CD34, CD11b,

CD19 and HLA-DR are not usually expressed by MSCs (negative markers), and antibodies for these were used to reveal contaminations. Cell dissociation, was carried out, and cells were pelleted by centrifugation at 400 G for 3 minutes at 4 °C. Cells were washed twice in cold stain buffer, used to maintain cell viability and maximize fluorescence signal intensities, and counted before another centrifugation. The cells were resuspended in the buffer to a concentration of approximately 5 x 10^6 cells/ml.
Tubes were arranged as following:

- 100 µl of the cell suspension was added to 14 tubes
- Antibodies for CD90, CD44, CD105, CD73, CD106, CD146 and CD166 were added to each their tube of cells (8 tubes)
- Positive and negative isotype control cocktails for human MSCs (hMSC) were added to one tube
- Positive and negative cocktail for human MSCs (hMSC) were added to one tube
- A smaller amount of isotype control (drop in) was added to one tube
- Isotype control for CD106, CD146 and CD166 were added to one tube
- hMSC positive cocktail and antibody for CD44 were added to one tube
- One tube was for cells only

During a 30-minute ice cold incubation in the dark (using aluminum foil), the tubes were frequently mixed with a vortex. The suspensions were further washed with cold stain buffer following cell dissociation and centrifugation at 400 G for 3 minutes. The pellets were resuspended in 500 µl of cold stain buffer and transferred to appropriate tubes for flow cytometry. Further specifications due to the protocol were followed in detail. Characterization of MSCs was carried out by Ph.D. candidate Ashraful Islam.

3.4.2 Isolation of MUSE-cells by Fluorescence-Activated Cell Sorting (FACS)

An antibody for the pluripotent marker SSEA-3 was used to distinguishing and sort out MUSE-cells from cultures of MSCs. NTERA-2 cells, used as positive control for SSEA-3, are also known to be SSEA-4^+ (70). Therefore, we wanted to check whether sorting and expansion of SSEA-3^+ cells from MSCs also would result in enrichment of SSEA-4^+ cells. Initially, FACS buffer for washing was prepared to be as fresh as possible. MSCs between P4 and P11 was prepared for cell sorting at a confluency of approximately 100%, recommended in the published protocol for MUSE-sorting (55). Detachment of MSCs, centrifugation at 400G for 3 minutes and counting of cells (using a cell strainer) were carried out. Washing of

cells with FACS buffer, followed by centrifugation was done twice. The cells were resuspended in FACS buffer to a concentration of 1-5 x 10^6 cells/ml before adding 1-2 ml of PBS + HSA buffer, and kept on ice for 20 minutes. Five tubes were prepared, each with a concentration of $\leq$1 x 10^6 cell/100 µl in FACS buffer (if more than 5 x 10^6 cell were available, more tubes similar to tube 4 were prepared).

1. Cells (only)
2. Cells + secondary antibody for SSEA-3 (negative control)
3. Cells + secondary antibody for SSEA-4 (negative control)
4. Cells + primary antibody (SSEA-3) + secondary antibody (SSEA-3), for sorting
5. Cells + primary antibody (SSEA-4) + secondary antibody (SSEA-4)

Primary antibodies were added, followed by an hour of incubation on ice with intermediate pipette mixing (done gently to avoid cell damage). Washing and centrifugation were done twice, before an hour incubation of the secondary antibodies. For SSEA-3, a *FITC-conjugated goat anti-rat IgM* was used as secondary antibody, while an *Alexa Fluor ® 546* conjugated antibody was used for SSEA-4. Finally, a cell suspension of 300 µl was prepared for each of the tubes presented for the machine. A tube was also prepared with 1 ml of α-MEM for collecting of first-generation MUSE-cells, further planted in a T-25 vented flask and incubated at low O_2 to mimic the physiological environment. Cell attachment, culture expansion with change of medium (α-MEM + 10% FBS) every 3-4 days, and subculturing to bigger flasks was carried out. Characterization of second-generation MUSE-cells (similar to that of first-generation sorting) was done when the primarily sorted cells gained a confluency of 70% or higher.

3.5 Single-cell spheroids formation assay

To evaluate M-cluster formation in suspension culture, SSEA-3^+ cells were sorted (by FACS) into a tube containing 1 ml α-MEM + 10% FBS. From this, calculations for a limiting dilution (serial cell-suspension dilution) was done, in accordance to the number of cells sorted. Methylcellulose was mixed into the dilution medium with a ratio of 1:5 (800 µl α-MEM + FBS and 200 µl of methylcellulose) prior to planting in the wells of a 24-well low binding plate. Methylcellulose was used to keep single cells separated within the well. The plate was kept in a low O_2 cabinet and controlled daily. This was done from the SSEA-3^+ cells from HFP-MSCs, MC-MSCs and the NTERA-2 cell culture. The method is based on recommendations from the procedure published by Kuroda and Wakao et al. (55). According to this specific procedure, one can assume cluster formation after 7-10 days of culturing, and successful cluster formation can be concluded when they have a diameter >25 µm.

According to the number of cells sorted from each specimen (e.g. HFP-MSCs and MC-MSCs), we calculated and prepared a serial of dilutions studied on a 24-well low-binding plate (see fig. 18), e.g.;

- 10 000 cells/1000 µl
- 1 000 cells/1000 µl
- 100 cells/1000 µl
- 10 cells/1000 µl
- 1 cell/1000 µl

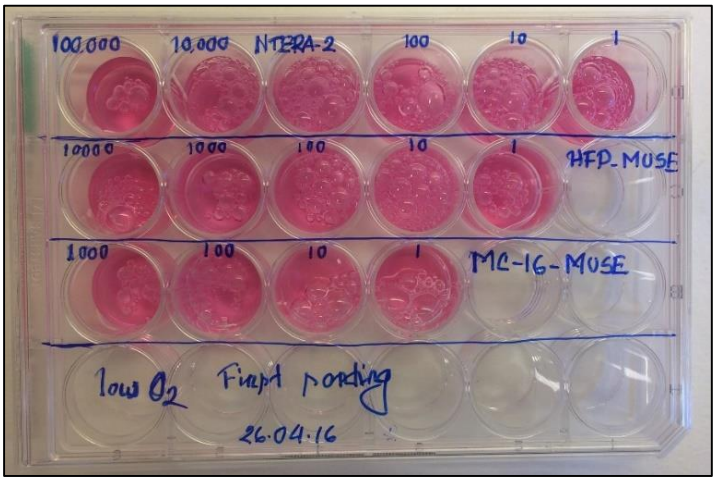

Figure 18. Limiting dilution for control of single-cell spheroids formation.

3.6 Chondrogenic differentiation assay in scaffold-free 3D spheroid culture

Cells in adherent culture are a poor resource for knowledge of tissue behavior. An appropriate recreation of the physiological environment is important for understanding AC disorders. 3D cell cultures are culturing techniques mimicking the *in vivo* environment, biochemically and physiologically. By introducing cells to an environment with low capacity for adhesion they tend to rather attach to each other. Therefore, stem cells in 3D culture makes spheroids. A simultaneously applied mixture of growth factors stimulates differentiation and cell-cell-interactions. Application of chondrogenic medium makes the stem cells differentiate into ECM producing chondrocytes. Chondrocyte spheroids are also called *chondrospheres* (27). There are several types of 3D culture methods, e.g. the hanging drop method (H.D.) or the conical well method (C.W., also called *the liquid overlay method*) (71). The C.W. method was used in this project, requiring 50 000 cells to make one spheroid.

96-well conical-bottom well plates (C.W.) were used to make single spheroids from adherent culture. Each of the wells has a volume of 150 µl. The plates were coated with the water-swellable polymer (hydrogel) poly(2-hydroxyethyl methacrylate) (Poly-HEMA) to inhibit cell adhesion (72). 1.2 g of Poly-HEMA was dissolved in 100 ml of 96% EtOH using a magnet stirrer at 50°C. Approximately 150 µl of the solution was applied to each of the C.W.-plates

used. These were kept in an incubator (60°C) for 24 hours for the alcohol to dry out, followed by aluminium foil covering and room temperature storage until use (up to three months). The wells were flushed with 150 µl of sterile PBS and the plate was placed in a heating cabinet for 1-2 hours before removing the buffer. They were further flushed with 150 µl sterile PBS and drained twice. Dissociation of confluent cells in adherent culture was carried out, including cell counting to find the number of cells/ml (# cells/ml) needed. The number of spheroids needed was depending on the tests we were supposed to use them for. Calculations of the volume needed to resuspend the pellet (V_{needed}) were done as following:

$$\#\ cells\ needed\ in\ total = \#\ cells/spheroid \cdot \#\ spheroids$$

$$V_{needed} = \frac{\#\ cells\ needed\ in\ total}{\#\ cells/ml}$$

$\#\ cells/spheroid$ = 50 000

The suspension was again centrifuged and the pellet was resuspended in the calculated volume needed. 150 µl of the cell suspension, holding approximately 50 000 cells, was transferred to single wells in the C.W.-plate to form single spheroids in these. The plate was centrifuged at 1100 xg for 10 minutes before placing it in a low O_2 incubator for 48 hours. By this time all of the spheroids were transferred to one well in a low binding plate (LBP). For this, a pipette with a sufficient sized end (e.g. a Pasteur pipette) was used to avoid damaging of the spheroids. Medium was removed from the wells of the LBP and replaced with 1 ml of pre-heated chondrogenic medium. Approximately 500 µl chondrogenic medium was replaced every 3-4 days. After 21 days in the LBP, the spheroids were transferred to Eppendorf tubes and flushed twice with PBS before fixating them with formalin for further testing.

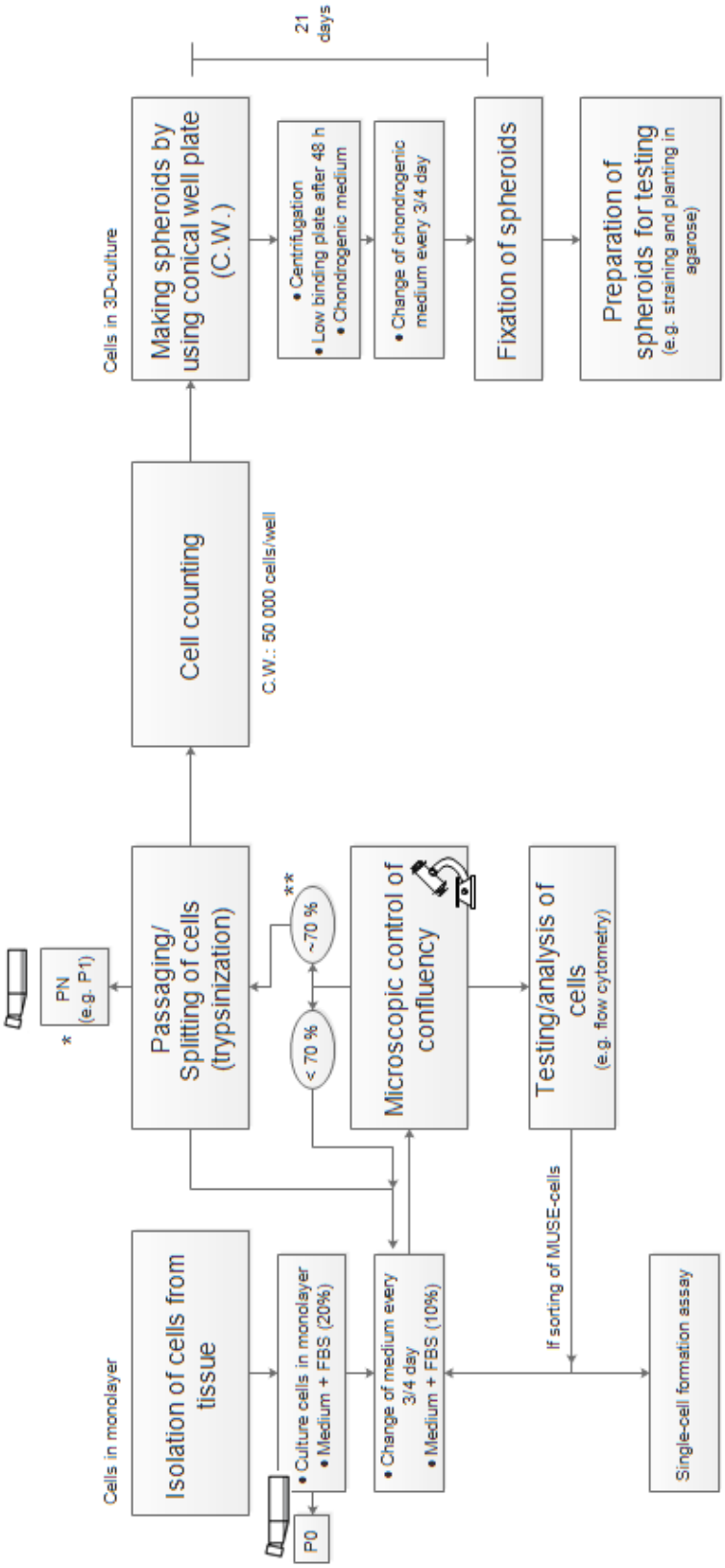

Figure 19. Overview of methods used. When frozen cells are being thawed for re-culturing, it is replacing the step "isolation of cells from tissue". PN is the referring to increase in passage number after spitting (*). "Passaging" also refers to freezing of cells. MSCs used for MUSE-sorting were expanded until ~100% confluency before cell dissociation, whereas MSCs used for spheroid formation were expanded until ~70% confluency (**). The picture was made by using the software Edraw Max 7.9 (01.05.16).

4 Results

4.1 Stem cell isolation from tissues and morphology of primary cultures

Isolation of stem cells from specimen of various tissues was done successfully in accordance to the methodology described. Simulation of a physiological environment with low risk of contamination was achieved by using incubators holding 37°C and a humidified atmosphere at 5% CO_2. Cells were cultured in either high (20%) or low (3%) O_2. The cells from HFP and MC were plastic-adherent and had a *fibroblast-like* morphology. Morphological comparison of MC-MSCs and HFP-MSCs is shown in fig. 20. Cells in P0 were starting to proliferate after attaching to the plate. Cells in early passage (P0) were proliferating slowly, needing approximately one week to gain a confluency of 70% with further passaging. Proliferation were higher with increased passage number (P3/4), needing only a few days upon next passage. The cells maintained their proliferative and plastic-adherent properties after recovery (thawing) from cryopreservation (liquid nitrogen). Cells of both HFP and MC appeared short in early passages, compared to a more elongated shape in later passages, like as if they are stretching for each other.

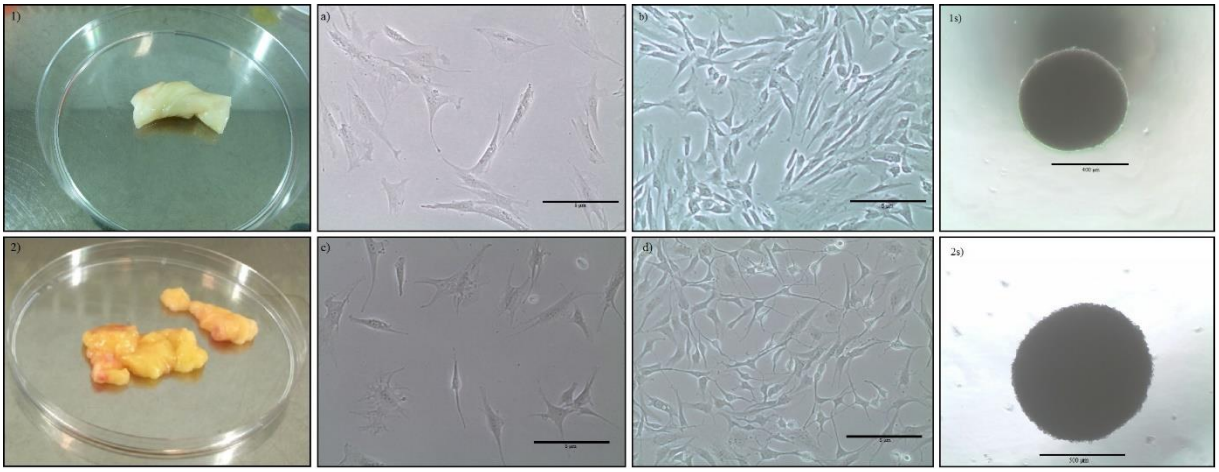

Figure 20. Morphological comparison of MSCs from MC (1) and HFP (2) in α-MEM. Attached MC-MSCs the day after planting in P2 (a), compared with 70-80% confluency in P3 (b). HFP-MSCs (P2) are attached to the growth plate one day after planting (c), compared to HFP-MSCs (P3) with ~70% confluency (d). MSCs from both MC and HFP exhibit a fibroblast-like elongated and bipolar shape. HFP-MSCs have a characteristic nodule core with slim extending poles. MC-MSCs are characteristically broader than HFP-MSCs along their entire length. Spheroids produced by MC-MSCs (1s, bar size = 400 µm) are characteristically smaller than those produced by HFP-MSCs (2s, bar size = 500 µm). Bar sizes in a-d = 5 µm.

4.2 Phenotypic characterization of isolated MSCs by flow cytometry

Isolated cells were analyzed for specific surface markers (clusters of differentiation, CD) by flow cytometry, in order to characterize their stem cell-like phenotype. The data was processed by using the computer software Flowjo, carried out by Ph.D. candidate Ashraful Islam. Fig. 21 represents the results in two-dimensional dot plots (top panels) and histograms, comparing HFP-MSCs and MC-MSCs analyzed at passage 3-4. Both cell types were positive for CD90, CD105 and CD73, as expected for MSCs. They were in addition positive for CD44, CD146 and CD166, markers related to differentiation potential. These were included because they may predict a differentiation potential towards a chondrogenic lineage (41). A very small amount of HFP-MSCs were positive for CD106, while this was slightly increased in MC-MSCs. A cocktail of antibodies specific for markers that usually are not expressed by MSCs (CD45, CD34, CD11b, CD19 and HLA-DR) was used to reveal potentially contamination of other cell types within the MSC population. This was nearly undetectable in both of the cell types, confirming that they, almost without exceptions, consisted of MSCs.

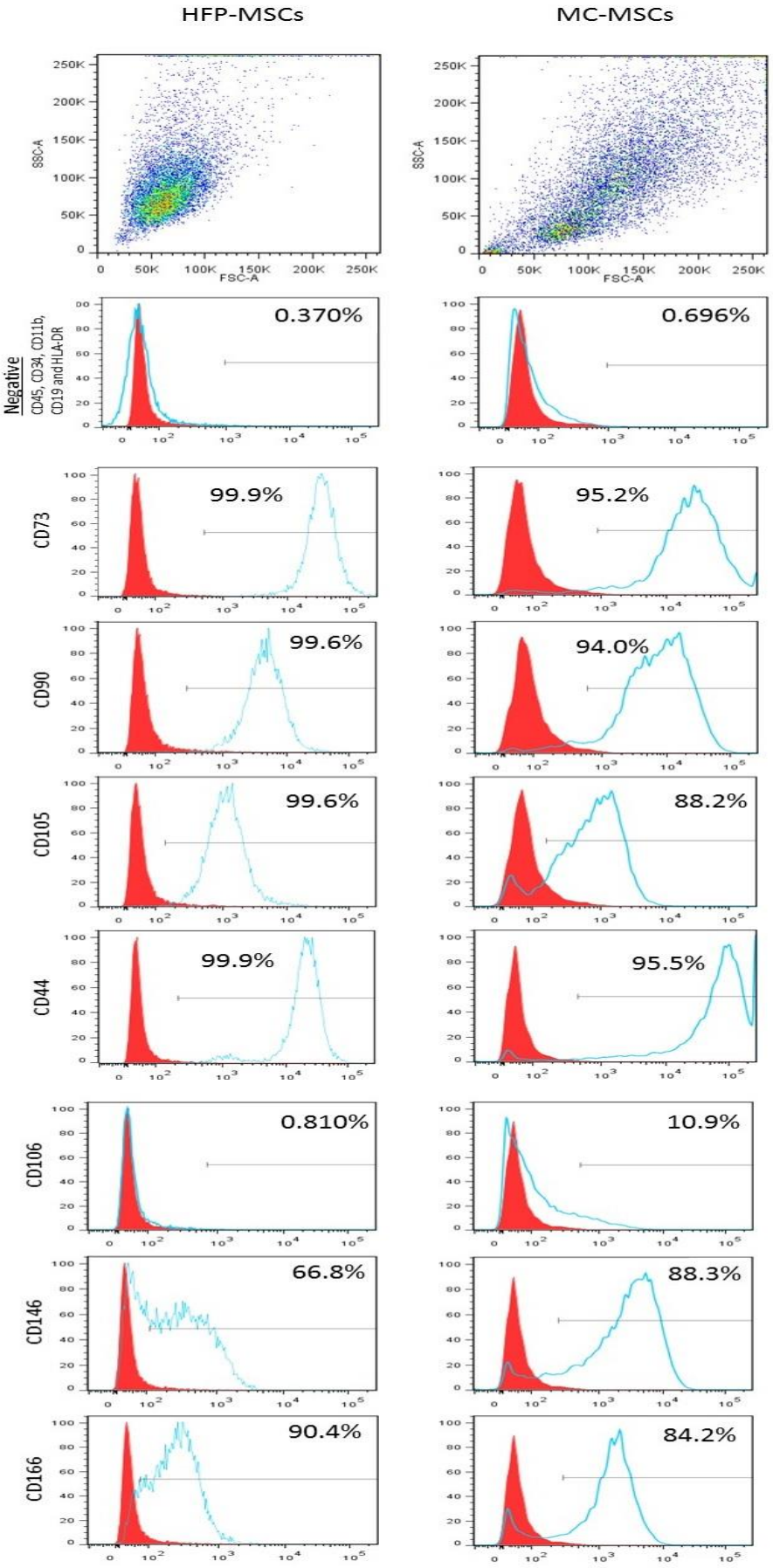

Figure 21. Phenotypic comparison of HFP-MSCs and MC-MSCs.

4.3 Chondrogenesis of HFP-MSCs and MC-MSCs

MSCs expanded in monolayer were used to make spheroids in scaffold-free three dimensional (3D) cultures. This was successfully done as described in the Methods section. The undifferentiated stem-like cells, after cell condensation, were treated with chondrogenic medium for 3 weeks to differentiate into chondrocytes. The spheroids seemed to attend a smoother shape after three weeks kept in suspension cultures with chondrogenic medium. Some of the spheroids (two to three) fused, making even bigger tissue-like structures. The cartilage-forming abilities were checked by Alcian blue staining assay. Saccharide-containing carboxyl groups in e.g. GAG molecules like HA are highlighted by the staining. Spheroids from HFP-MSCs were abundant in GAGs (dark blue stained area), with cells residing in distinct lacunae formation, similar to that of native cartilage. Spheroids from MC-MSCs had an almost absent blue staining, indicating low production of GAGs, and there were no signs of lacunae formation.

This is also evident in the spheroid composition. Similar to native cartilage, the superficial zone in the spheroids from HFP-MSCs are consisting of flattened and discoid shaped cells. In the deeper layers, the cells appear bigger and more round in shape. This is not the case for MC-MSCs, where the cells appear small and has no morphological relation to the layers of the ECM (fig. 22). Spheroids from MC-MSCs were smaller in size than those from HFP-MSCs (fig. 20). These findings indicate that MC display chondrogenesis, compared to HFP, which had the morphological resemblance of native cartilage.

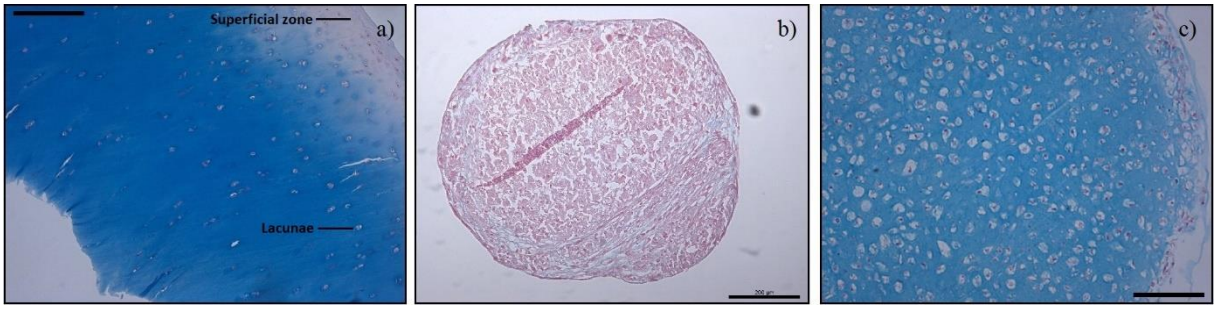

Figure 22. Alcian blue stained cartilage. Light microscopy of sectioned MC-MSCs spheroids (b) and HFP-MSCs spheroids (c) stained with Alcian blue solution reveals their chondrogenesis and ECM production. Alcian blue stained native articular cartilage (a) is here used for best comparability. HFP-MSCs presents abundant amounts of GAGs and lacunae-like structures, whereas MC-MSCs failed to produce such cartilage characteristics. The spheroids were conditioned in TGF-β_3- and BMP-2-enriched chondrogenic medium. The bars indicate 200 µm.

4.4 Culturing of NTERA-2 cells

An embryonic cell line (NTERA-2), which is known to expressing the SSEA-3 antigen, was used as positive control for the flow cytometry analysis. NTERA-2 cells are adherent to plastic but are characterized as *epithelial-like* cells. They are characteristically more compact than fibroblast-like cells and display a more polygonal shape. Of note, NTERA-2 cells are a cell line of genetically similar cells, while primary cultures of MSCs may be more heterogeneous. Culturing of these cells was done successfully, and carried out as for MSCs, in α-MEM + 10% FBS, except the addition of bFGF. The cells were highly proliferative and could gain a confluency of 80-90% in only a couple of days. Therefore, we needed to control confluency of these cells regularly. In adherent culture, the cells characteristically grew in cluster formation. During passaging from confluent state, they were easily detached from flask, in comparison to MSCs. Fig. 23 show the morphology of NTERA-2 cells. The cells were viable when thawed from frozen state (liquid nitrogen), although, compared to MSCs used, a greater amount appeared non-viable when planted.

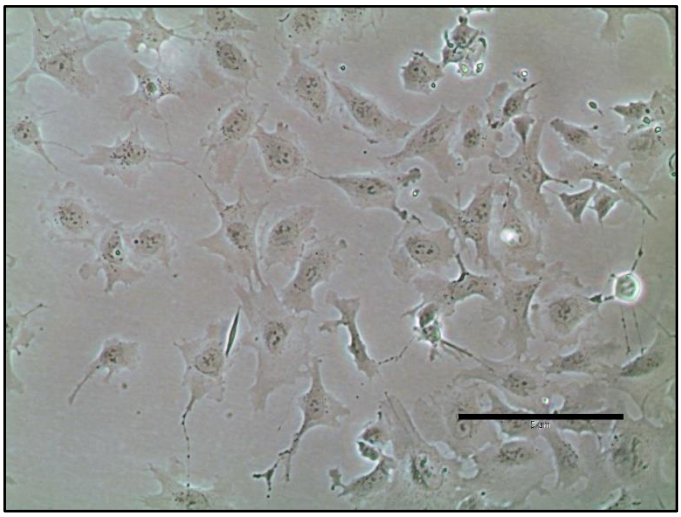

Figure 23. NTERA-2 cells. The figure shows cells two days after planting in P2. The EC cells are quickly proliferating and are characteristically gaining confluency from clusters formatted in monolayer (not shown here). The bar indicates 5 µm.

4.5 Isolation of SSEA-3$^+$ MUSE-cells from MC-MSCs and HFP-MSCs

Isolation of MUSE-cells from MSC cultures were carried out by FACS in two rounds. MUSE-cells are SSEA-3/CD105 double positive, whilst CD105 is a phenotypic marker for MSCs. The phenotypic characterization of both MC-MSCs and HFP-MSCs confirmed a global positive expression of CD105 (fig. 21). Therefore, sorting (primary analysis) was carried out for SSEA-3$^+$ cells. NTERA-2 cells (positive control), HFP-MSCs and MC-MSCs were expanded in monolayer to a passage between P4 and P11 (P4, P4 and P6, respect-ively). Further, sample preparations for FACS were done, as described in the Method section. When cell suspensions were presented to the BD FACSAria III, data were processed and micrographs generated (fig. 24). The NTERA-2 cell culture, which is known positive for this marker, comprised of 22.3% SSEA-3$^+$ cells. 8.22% of the cells in the HFP-MSC culture and 0.894% of MC-MSCs expressed SSEA-3. These fractions were sorted and further expanded in monolayer culture. MUSE-cells are, as described in previous publications, morphologically undistinguishable from MSCs in a heterogeneous MSC population (55). Fig. 25 shows isolated SSEA-3$^+$ cells from HFP (MUSE) compared to the MSC population they were derived from. An interesting observation is the elongated shape of HFP-MUSE-cells after attachment and expansion. Of notice, both MSCs and MUSE-cells were expanded in the presence of bFGF.

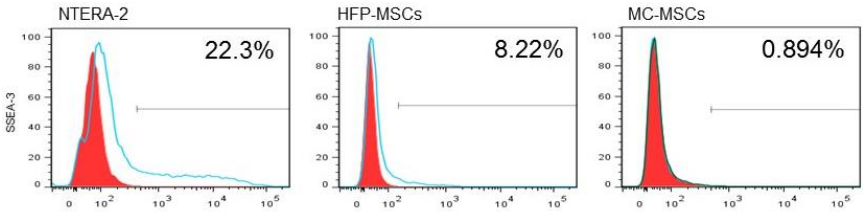

Figure 24. First characterization of SSEA-3 expression. Primary characterization of SSEA-3$^+$ cells in HFP-MSCs and MC-MSCs compared to NTERA-2 cells. 22.3% of the NTERA-2 cell population is SSEA-3$^+$. The expression is present in 8.22% of the HFP-MSCs and in 0.894% of the MC-MSCs.

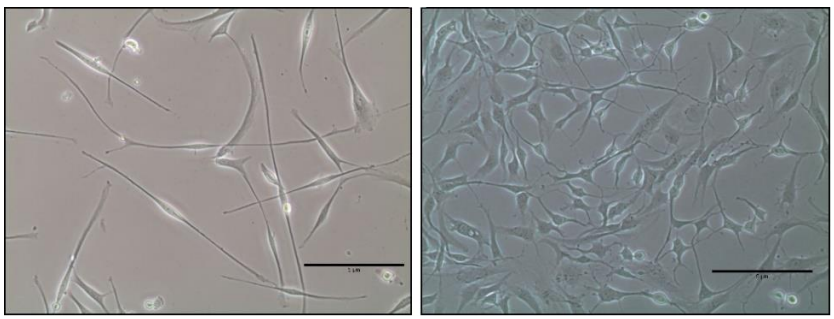

Figure 25. Comparison of isolated SSEA-3$^+$ cells and regular MSCs. HFP-MUSE cells are undistinguishable from HFP-MSCs (right) in a confluent state. However, after treating with bFGF, MUSE-cells appeared especially elongated in early expansion culture (left). This may, however, just be a coincident. The bars indicate 5 µm.

4.6 Phenotypic characterization of isolated MUSE-cells

SSEA-3^{+} cells were sorted from the mix MSC cultures and further expanded in monolayers until reaching a sufficient number of cells (1-2 passages) for *secondary* analysis (characterization). Enrichment of the SSEA-3^{+} fraction after the second flow cytometry would confirm the correct positive selection done during the first analysis. Results indicated a significant enrichment of SSEA-3 expression in HFP-MUSE cells (50% vs. 8%), pointing out that most of the originally selected cells had been able to undergo self-renewal. By this, we could conclude that a correct selection of cells was done phenotypically. On the other hand, characterization of MC-MUSE cells presented a slightly decrease in SSEA-3 expression, compared to the primary analysis (respectively 0.336% vs. 0.894%), indicating an unsuccessful selection of cells. Fig. 26 represent the SSEA-3 expression in HFP-MSCs and MC-MSCs compared to NTERA-2 cells.

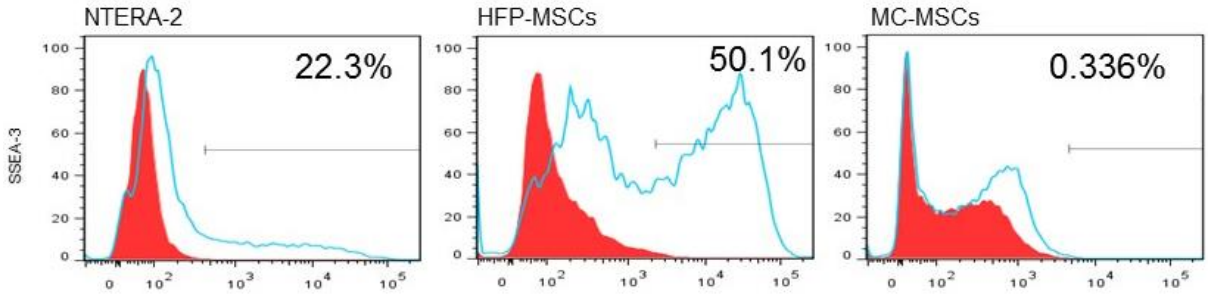

Figure 26. Second characterization of SSEA-3 expression. Secondary characterization of SSEA-3^{+} cells from HFP-MSCs and MC-MSCs, compared to NTERA-2 cells. 22.3% of the NTERA-2 cell population is SSEA-3^{+}. The expression is present in 50.1% of the HFP-MSCs and in 0.336% of the MC-MSCs.

4.6.1 Characterization of the pluripotency marker SSEA-4

Since we chose to use the embryonic carcinoma (EC) NTERA-2 cells as positive control for the expression of SSEA-3 in our cultures (HFP and MC), we came up with the idea to test for the embryonic marker SSEA-4, expressed by both pluripotent ECs and ESCs (70). This was conducted to see if sorting and expansion of SSEA-3^+ cells also would result in enrichment of SSEA-4^+ cells (if the expression of the two pluripotency markers were related). Of notice, MUSE-cells are not known to be SSEA-4^+. The characterization of SSEA-4 was carried out simultaneously with SSEA-3 characterization, during both primary and secondary analysis. Interesting, approximately 50% of the MSCs derived from both HFP and MC expressed SSEA-4 in the primary characterization. For the second characterization, SSEA-3^+ cells isolated and expanded from HFP exhibited an increase in the expression of SSEA-4 (>90%), being more similar to that of NTERA-2 cells (>80%). On the other hand, SSEA-3^+ cells isolated from MC exhibited a shift towards reduction in the expression of SSEA-4 (13%). This is shown in fig. 27. Table 5 compares the expression of SSEA-3 and SSEA-4 in the primary and secondary characterization of NTERA-2 cells, HFP-MSCs and MC-MSCs.

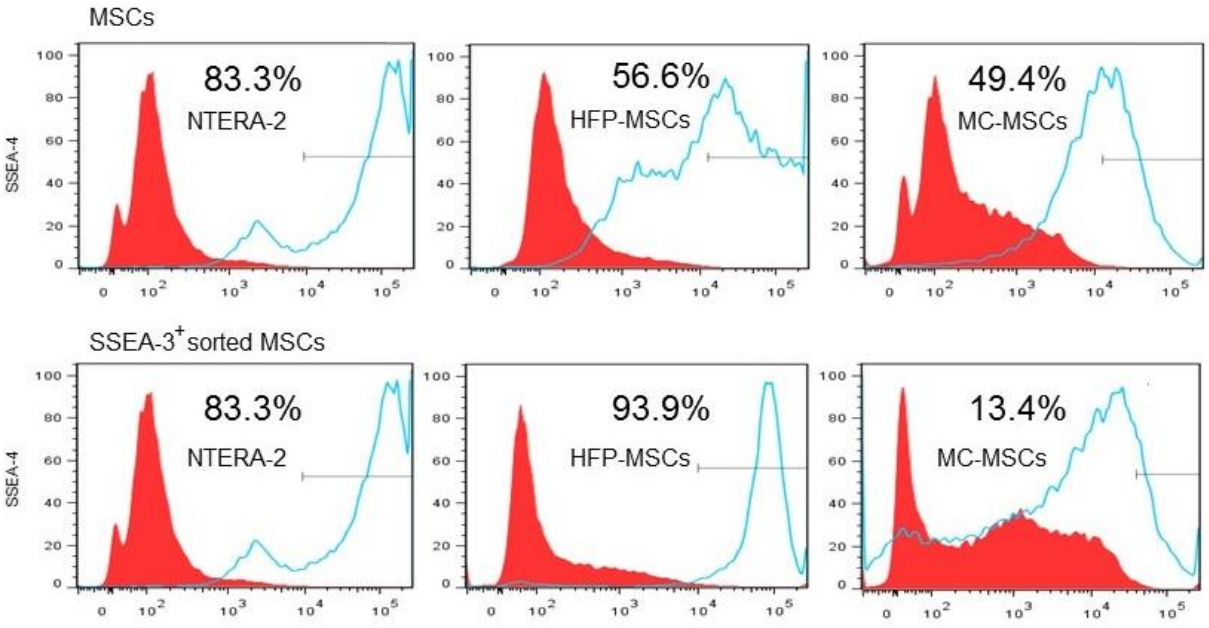

Figure 27. Characterization of SSEA-4 expression. Expression of SSEA-4 in HFP- and MC-MSCs, characterized during MUSE-cell isolation (primary analysis), compared to the characterization of expanded SSEA-3^+ cells (secondary analysis). In both cases, NTERA-2 cells were used as reference.

Table 5. Overview of flow cytometric characterization of cells. The table shows characterization and sorting of SSEA-3^+ cells from a certain passage number between P4 and P11 (primary analysis), and characterization after sufficient expansion of these cells (secondary analysis). All the specimens were kept in a low O_2 incubator, similar to the physiological environment of cartilage. For secondary analysis, the samples are named e.g. "MUSE/MC-MSCs" to display the passage number of SSEA-3^+ sorted cells, in comparison to the original culture. However, for the case of MC-MSCs, MUSE-cell sorting was not successful (inappropriate to call them MUSE-cells).

Primary analysis				*Secondary analysis*			
Sample	Passage	SSEA-3^+	SSEA-4^+	Sample	Passage	SSEA-3^+	SSEA-4^+
NTERA-2	P4	22.3%	83.3%	–	–	–	–
HFP-MSCs	P4	8.22%	56.6%	MUSE/HFP-MSCs	P4/P9	50.1%	93.9%
MC-MSC	P6	0.894%	49.4%	MUSE/MC-MSCs	P4/P11	0.336%	13.4%

4.7 Functional characterization of SSEA-3^+ MUSE-cells

The single-cell cluster formation assay by limiting dilution (methyl cellulose culture) was successfully from the HFP-MSC culture. As expected and described by Wakao et al., cells formed clusters similar to embryoid bodies from ESCs after approximately 7 days in suspension culture (fig. 28) (52, 55). This was only a trial to test if the procedure was working, and number spheroids formed was not inspected.

Figure 28. Single-cell spheroid formation. After limiting dilution, single cells are kept separated by methylcellulose (a). After 7 days in culture, clusters from single cells were detected (b and c [magnification of b in c]). Bars indicates: a = 5 µm, b = 5 µm, c = 50 µm.

4.8 Chondrogenic potential of MUSE-cells

A number of experimental hindrances at the beginning of the project were delaying the acquisition of relevant data. In addition, the experimental settings in this project, starting from the initial cell isolation, cell expansion, sorting and chondrogenic differentiation is lengthy and very laborious. Because of the named circumstances, the final comparison of chondrogenic potential between MUSE- and non-MUSE-cells could not be finalized at the time of delivering the essay. We expect to have preliminary results on this at the time of the oral exam.

5 Discussion

In this project we carried out procedures for isolation of MSCs from HFPs and UCs. In chondrogenic assays we demonstrated that HFP-MSCs had higher differentiation potential towards cartilage than MC-MSCs. Additionally, a fraction of SSEA-3^+ MUSE-cells could be isolated from both NTERA-2 cells and HFP-MSCs, but not from MC-MSCs. Isolated MUSE-cells were highly positive for the SSEA-3 marker after the second cell expansion and were able to form cluster from single cells.

The main achievements and findings of this work are:

1) MSCs were successfully isolated from HFP and MC
2) HFP-MSCs display better chondrogenic potential (and abilities) than MC-MSCs
3) SSEA-3^+ MUSE-cells were successfully isolated from HFP-MSCs, but not from MC-MSCs
4) HFP-MUSE cells were able to form single-cell spheroids
5) Chondrogenic potential of MUSE-cells vs. non-MUSE-cells is under investigation

5.1 Isolation and characterization of MSCs from HFP and MC

By characterization of stem-like cells from HFP and MC, we prove these to be MSCs. They were positive for the characteristic MSC markers CD90, CD73 and CD105. They also expressed the differentiation-related markers CD44, CD146 and CD166, telling that these cells could have a potential to undergo chondrogenic differentiation. Expressions of CD45, CD34, CD11b, CD19 and HLA-DR were, as expected, absent. MC-MSCs had a slightly different expression of the following markers, in comparison to HFP-MSCs:
Higher expression of CD106 (10.9% vs. 0.810%) and CD146 (88.3% vs. 66.8%), and lower expression of CD105 (88.2% vs. 99.6%). The positive expression of CD146 in MC-MSCs (compared to HFP-MSCs) are concurring with previous findings in our research group (41). Another study reported of a subpopulation $CD106^+$ cells within UC-MSCs (7.44%), having increased immunomodulatory properties (73). Compiling these findings of increased expressions (CD106 and CD146) with the down-regulated expression of CD105, being a known marker expressed by MSCs, there are indications of a subtype of cells distinct from MSCs within the MC-MSC population.

5.2 Chondrogenesis of HFP- and MC-MSCs

In this study, we demonstrated that HFP-MSCs make better cartilage spheroids than MC-MSCs. The use of MC or cord compartments for cartilage regeneration are still controversial. A few studies are presenting MC-MSCs as a potential good source of MSCs to undergo chondrogenesis (49), while others are presenting a poor potential (74). However, most studies have been focusing on umbilical cord blood (UCB) (75-77). In our study, Alcian blue staining revealed lacunae formation, abundant production of GAGs and zonal arrangement in HFP-MSCs, similar to that of native cartilage. MC-MSCs did not display any of these characteristics. Differences in outcomes may be due to changes in isolation, expansion or chondrogenic protocols. In addition, the criteria for defining chondrogenesis and cartilage-like tissue formation is different between studies. Despite the many positive sides of using MC-MSCs for transplantation strategies, caution should be taken while considering this cell source for cartilage repair.

5.3 Isolation and characterization of MUSE-cells from HFP- and MC-MSCs

Our study is the first to test the isolation capacity of MUSE-cells from HFP and MC. We demonstrated that the adipose tissue of HFP could contribute with approximately 8% MUSE-cells, while MC had close to 0% of these cells. Thereby, HFP appeared to be a good source for MUSE-cells, while MC appeared to be a bad source of these cells. Human sources that one previously has demonstrated MUSE-cell isolation from, is BM (aspirate), AT (lipo-suction), dermis fibroblasts, in addition to commercially available BM-MSCs, fibroblasts and AT-MSCs (53-57, 78-82). Recently, they have also been successfully isolated from goat skin fibroblasts (83, 84). Among the sources MUSE-cells so far have been isolated from, adipose tissue-derived MUSE-cells (MUSE-AT) appear as the most promising for appliance in regenerative medicine (78). An interesting finding in our study is that the number of HFP-MUSE cells seem to be correlated with the previously reported number of MUSE-cells in adipose tissue (MUSE-AT), collected by lipoaspiration from the abdominal cavity, 8.8% $\pm$ 1.3% (80). Further, the results can be compared to BM-MSCs, reported to a hold up to 5-6% of these cells (52, 53). Sorting and expansion of these cells resulted in an increase of SSEA-3^+ cells up to ~50%, indicating the ability to undergo self-renewal. Even though MC-MSCs consisted of only 0.8-0.9% SSEA-3^+ cells, the number is still concurrent with the 1-2% reported in dermal fibroblasts, or the vanishingly low 0.03% reported in mononuclear cells from BM (53, 85). However, this sorted fraction of cells (MC-MSCs) did not manage to

undergo self-renewal, yielding a population of only 0.336% after second cell expansion, indicating residual sorting of cells in an unspecific way.

In a trial conducted at the very end of this master project, we demonstrated that HFP-derived MUSE-cells were able to form embryo-like clusters in suspension culture. Their ability to survive and proliferate in suspension, similar to ESCs, is often described in prior to transfer onto a gelatin-coated dish, where they spontaneously differentiate into cells expressing markers characteristic to all the three germ layers (triploblastic differentiation) (55). This triploblastic differentiation (*in vitro*) potential will be further studied in our group. AC is another example of a tissue not yet demonstrated to hold MUSE-cells. In our laboratory we are investigating the potential presence of MUSE-cells in cartilage. Preliminary results from this week revealed a 7-8% fraction of cells positive for SSEA-3. Furthermore, characterization of the differentiation and repair potential of MUSE-cells has also been described is animal studies (*in vivo*). An example of local application is transplantation of melanocyte induced MUSE-cells (in vitro medium induction) into the skin of immunodeficient mice. Such models have been used in all *in vivo*-studies of MUSE-cells, showing non-tumorigenicity (when transplanted into testes) and no immunorejection (52, 56). Other animal studies have tested the impact of MUSE-cells in e.g. liver damage, skin damage, muscle degeneration and spinal cord injury after infusion into the peripheral bloodstream (53). Therefore, it is important to fulfill the procedures for MUSE-characteri-zation by conducting tests for *in vitro* and *in vivo* differentiation capacities for all new specimen tested (e.g. HFP and AC chondrocytes). In summary, the process should be lined up as following; isolation from tissue – single-cell spheroid formation – *in vitro* differentiation capacities (spontaneously and medium induced) – *in vivo* (animal) studies (pre- or un-differentiated).

Of notice, we only managed to process one sample of each tissue (HFP and MC) during the project period, due to certain practical problems. Therefore, we cannot for certain conclude favorable tissue source (HFP or MC) for MUSE-cells until more parallels have been conducted. However, there is a pattern indicating that HFP is the best of these two sources, both because of the ability to form better cartilage-like constructs in 3D culture than MC, and because of the higher levels of MUSE-cells within the MSC population. Because of a complex protocol, there are always sources of error that might have resulted in these findings, considering MCs (55). A schematically protocol for MUSE-cell sorting is presented in Appendix C.

BM aspirate contains cell types like BM-MSCs and hematopoietic stem cells (HSCs). Both BM-HSC and BM-MSC fractions contains mononuclear cells, from which MUSE-cells previously have been isolated from (53). There are, however, no reports of MUSE-cell isolation from blood. Therefore, MUSE-isolation from blood, e.g. MSC-containing blood of the umbilical cord (UCB) should be investigated (86). Further studies should be done to make a final conclusion of UC as a source for MUSE-cells, and hence its possible use in cartilage regeneration. In the future, MUSE-cells could be of extensive use in stem cell banks, due to their broad specter of possible applications in regenerative medicine (78).

5.4 Chondrogenesis of MUSE-cells

To date, no studies have addressed the chondrogenic differentiation potential of MUSE-cells. Additionally, there has not been any attempts to use MUSE-cells for regenerative medicine in cartilage repair or joint disorders. The plan for this project was mainly to isolate MUSE-cells from UCs and HFPs, test their chondrogenesis in 3D culture, for so to compare this property between MUSE- and non-MUSE-cells of each tissue specimen. However, due to lack of time and unforeseen practical problems, my participation to this project ended before we managed to test chondrogenic potential of MUSE-cells.

Chondrocytes, adipocytes and osteocytes are example of cells from the mesodermal lineage (53). Since MUSE-cells reside in MSC populations, it is expected that they are able to undergo chondrogenic differentiation, because MSCs themselves have this ability (53). The cells have also been reported to favorably differentiate into cells of the mesodermal lineage, compared to the lineages of ectoderm and endoderm. MUSE-cells have been reported to differentiate into several cell lineages (*in vivo* and *in vitro*), both spontaneously and through medium/cytokine induction (Appendix D) (52-54, 56). Adipocyte- and myocyte induction medium pushed the cells towards adipocytes and myocytes (both of mesodermal lineage), respectively, in shorter time span then compared to MSCs (57). Induced differentiation towards osteoblasts (expressing osteocalcin) has also been conducted *in vitro* (54). These are strong indications for a potential to undergo chondrogenic differentiation, and perhaps more efficiently than MSCs (3 weeks). Good chondrogenesis of cells from HFP (contains MUSE-cells), compared to poor chondrogenesis of MC cells (lacking MUSE-cells), could in such a case be explained by the contribution of MUSE-cells. MUSE-cells has also been induced towards melanocytes, hepatocytes (and biliary cells) and neural cells using growth factor enriched medium, similar to medias used for *in vitro* differentiation of other stem cells (e.g.

melanocyte differentiation media containing bFGF, ITS and others) (54, 56, 57). Since they are able to become neural cells (*in vivo* and *in vitro*), they might play an important role in treatment of diseases like multiple sclerosis or Alzheimer (53, 54, 57). They might even be important in fight several types of cancer. Stem cells used in regenerative medicine have an overall low survival rate, due to high environmental stress, indicating the need of such stress-enduring cells (79).

5.4.1 Potential use of MUSE-cells in clinical settings

Undifferentiated MUSE-cells may as well be beneficial for engraftment into an inflamed joint, because of their stress tolerance, downregulated expression of genes for cell death and survival, and upregulated expression of genes related to DNA repair (57, 79). They seem to grow fine in low O_2 (*in vitro*), representing the environment in AC. In potential application to joints, the cells most certainly need to be applied locally, since the tissue lacks vascularization (cells are not able to home towards the site of damage through injection in the peripheral bloodstream). It might be that HFP, even though it is an adipose tissue, is more suitable for chondrogenic differentiation compared to abdominal fat, due to its relation to cartilage in the joint (environmental similarity) (57). Of importance, it has been demonstrated that HFP-MSCs show superior chondrogenic potential, in comparison to AT-MSCs (87).
Some of the factors that MSCs produce are immunomodulatory and has an anti-inflammatory effect (40). When it comes to UC-MSCs, it has been shown that their low immunogenicity and immunosuppressive effects may decrease the risk of GvHD (38). MSCs from any donor source seem to suppress T-cell proliferation ($CD4^+$ and $CD8^+$), abrogate memory T-cells to their antigen, and reduce the expression of certain activation markers. Furthermore, a variety of other immunomodulatory pathways have been described (88). In MSC populations, non-MUSE-cells may play a role in exerting trophic and immunosuppressive effects, while MUSE-cells mainly work as “tissue repair” cells, able to home for damaged tissues and undergo triploblastic differentiation (40). Because of MSCs abilities to downregulate/suppress these kinds of reactions *in vitro* (immunomodulation), they’ve been considered *immune privileged*, or *immune evasive* as they are more recently called (41, 89). However, there are no known experimental records of MUSE-cell having anti-inflammatory or immunoregulatory abilities, and more knowledge of the synergy between MUSE- and non-MUSE-cells is needed to understand their biology in conditions of stress, injury or inflammation (the recipient site is a harsh environment) (57). In disease management, MUSE-cells and non-MUSE-cells may be considered applied in certain mix ratios (since MUSE-cells seem to work “repairing” and non-

MUSE-cells are immunomodulatory, among others) (53). As an avascular and non-lymphatic tissue, it would be natural to imagined AC as a site of immunoprivilege. Nevertheless, a recent *in vivo* study (allo- and xenografts in rabbit knee) discovered immunoprivilege in cartilage to be dependent on donor source and lesion location (90).

6 Conclusions

In this project, we demonstrate that the adipose tissue of HFP is a good source for MSCs, able to produce good cartilage-like constructs (chondrogenic potential) and harbor a subpopulation of SSEA-3^+ MUSE-cells. We managed to establish general protocols for isolation and characterization of MSCs and MUSE-cells. However, MSCs derived from MC produced bad cartilage spheroids and were a poor source for SSEA-3^+ MUSE-cells. Therefore, our initial hypothesis was partially not validated by this study. We also discovered an expression of SSEA-4^+ cells within both MSC cultures. However, only cultures of cells sorted positive for SSEA-3 were able to self-renew (HFP-MSCs) and increase the expression of both SSEA-3 and -4. HFP-MUSE-cells were also able to produce embryonic-like single-cell spheroids. Comparative studies related to the chondrogenic potential of MUSE- vs. non-MUSE-cells from HFP-MSCs are at this moment ongoing.

7 Future aspects

This study has put forward that umbilical cords (the solid parts) are not a good source of MUSE-cells. However, other tissues from the joint could represent rich sources of MUSE-cells. If the chondrogenic capacity of HFP-MSCs is linked to the presence of SSEA-3^+ MUSE-cells, and/or if MUSE-cells are superior in making cartilage than the whole bulk of MSCs, the use of MUSE-cells for cartilage reconstruction or for the treatment of cartilage degenerative disorders such as OA should be seriously considered.

At our laboratory we are at the moment comparing the chondrogenic potential of MUSE- vs. non-MUSE-cells. We are also checking the proportion of MUSE-cells in other joint tissues, such as cartilage and synovial membrane. In parallel, we are investigating other methods for isolation of MUSE-cells from tissues based on resistance to harsh enzymatic treatment.

If these efforts would turn positive, we should move to *in vivo* animal studies to check the reparative capacity of MUSE-cells, both in focal cartilage repair models and in OA models.

References

1. Swales C, Bulstrode C, Bulstrode CJK. Rheumatoid arthritis. In: Rheumatology, orthopaedics and trauma at a glance. 2nd ed. Chichester: Wiley-Blackwell; 2012. p. 54.

2. Grotle M, Hagen KB, Natvig B, Dahl FA, Kvien TK. Prevalence and burden of osteoarthritis: results from a population survey in Norway. Journal of Rheumatology. 2008 Apr;35(4):677-84.

3. Zhang Y, Jordan JM. Epidemiology of Osteoarthritis. Clinics in Geriatric Medicine. 2010 Aug;26(3):355-69.

4. Kvien TK, Glennas A, Knudsrod OG, Smedstad LM, Mowinckel P, Forre O. The prevalence and severity of rheumatoid arthritis in Oslo. Results from a county register and a population survey. Scandinavian Journal of Rheumatology. 1997 Aug;26(6):412-8.

5. Smeltzer SCOC, Brunner LS, Suddarth DS. Musculoskeletal function. In: Smeltzer SCOC, Brunner LS, Suddarth DS, editors. Brunner & Suddarth's textbook of medical-surgical nursing: Vol 1. 12th ed. Philadelphia: Wolters Kluwer/Lippincott Williams & Wilkins; 2010. p. 2011.

6. Clouet J, Vinatier C, Merceron C, Pot-vaucel M, Maugars Y, Weiss P, et al. From osteoarthritis treatments to future regenerative therapies for cartilage. Drug Discovery Today. 2009 Oct;14(19–20):913-25.

7. Smith MD. The Normal Synovium. The Open Rheumatology Journal. 2011 Oct;5:100-6.

8. Sophia Fox AJ, Bedi A, Rodeo SA. The Basic Science of Articular Cartilage: Structure, Composition, and Function. Sports Health. 2009 Nov;1(6):461-8.

9. Jay GD, Britt DE, Cha CJ. Lubricin is a product of megakaryocyte stimulating factor gene expression by human synovial fibroblasts. Journal of Rheumatology. 2000 Mar;27(3):594-600.

10. Classification of joints [Internet] Houston Texas, USA: RICE university; 2013 [cited 2016.03.09]. Available from: https://cnx.org/contents/3-29HBBo@3/Classification-of-Joints.

11. Peckham M. Cartilage. In: Histology at a glance. Chichester: Wiley-Blackwell; 2011. p. 38-9.

12. Lane NE, Wallace DJ. Cartilage and Its Accomplices The Body's Shock Absorbers. In: Bossert J, Wallace J, editors. All about Osteoarthritis: The Definitive Resource for Arthritis Patients and Their Families. Cary, USA: Oxford University Press, Incorporated; 2002. p. 30.

13. Huether SE, McCance KL. Disorders of Joints. In: Brashers VL, Rote NS, editors. Pathophysiology: the biologic basis for disease in adults and children. 7th ed. Missouri, USA: Mosby Elsevier; 2014. p. 1565-8.

14. Zhang L, Hu J, Athanasiou KA. The Role of Tissue Engineering in Articular Cartilage Repair and Regeneration. Critical Reviews in Biomedical Engineering. 2009;37(1-2):1-57.

15. Goldring MB. Chondrogenesis, chondrocyte differentiation, and articular cartilage metabolism in health and osteoarthritis. Therapeutic Advances in Musculoskeletal Disease. 2012 Aug;4(4):269-85.

16. Nelson DL, Lehninger AL, Cox MM. Carbohydrates and Glycobiology. In: Ahr KR, Randi, editor. Lehninger principles of biochemistry. 5th ed. New York: Freeman; 2008. p. 254-5.

17. Chen FH, Rousche KT, Tuan RS. Technology Insight: adult stem cells in cartilage regeneration and tissue engineering. Nature Clinical Practice: Rheumatology. 2006 Jul;2(7):373-82.

18. Tang X, Fan L, Pei M, Zeng L, Ge Z. Evolving concepts of chondrogenic differentiation: history, state-of-the-art and future perspectives. European Cells & Materials. 2015 Jul;30:12-27.

19. Zuscik MJ, Hilton MJ, Zhang X, Chen D, O'Keefe RJ. Regulation of chondrogenesis and chondrocyte differentiation by stress. Journal of Clinical Investigation. 2008 Feb;118(2):429.

20. Sherwood L. Principles of Endocrinology; The Central Endocrine Glands. In: Alexander S, Glubka A, editors. Introduction to human physiology. 8th ed. Independence, USA: Cengage Learning; 2013. p. 709.

21. Chen-An P, Andreassen KV, Henriksen K, Karsdal MA, Bay-Jensen A-C. Investigation of chondrocyte hypertrophy and cartilage calcification in a full-depth articular cartilage explants model. Rheumatology International. 2012 Mar;33(2):401-11.

22. Page-McCaw A, Ewald AJ, Werb Z. Matrix metalloproteinases and the regulation of tissue remodelling. Nature Reviews: Molecular Cell Biology. 2007 Mar;8(3):221-33.

23. Umlauf D, Frank S, Pap T, Bertrand J. Cartilage biology, pathology, and repair. Cellular and Molecular Life Sciences. 2010 Aug;67(24):4197-211.

24. Porter S, Clark IM, Kevorkian L, Edwards DR. The ADAMTS metalloproteinases. Biochemical Journal. 2005 Feb;386(1):15-27.

25. Swales C, Bulstrode C. Pathogenesis of rheumatoid arthritis. In: Rheumatology, orthopaedics and trauma at a glance. 2nd ed. Chichester: Wiley-Blackwell; 2012. p. 52-3.

26. Luks H. Cartilage Injury and Cartilage Defects [Internet] New York, USA: Howard J. Luks, MD.; 2014 [cited 2016.04.12]. Available from: http://www.howardluksmd.com/education/common-injuries/cartilage-defects/.

27. Makris EA, Gomoll AH, Malizos KN, Hu JC, Athanasiou KA. Repair and tissue engineering techniques for articular cartilage. Nature Reviews: Rheumatology. 2015 Jan;11(1):21-34.

28. Lories RJ, Luyten FP. Osteoarthritis, a disease bridging development and regeneration. BoneKEy Reports. 2012 Aug;1:136.

29. Playfair JHL, Chain BM. Transplant rejection. In: Immunology at a glance. At a glance series. 10th ed. Chichester: Wiley-Blackwell; 2013. p. 86-7.

30. Polacek M. The secretome of cartilage, chondrocytes and chondroprogenitors: implications for cell transplantation strategies [Doctoral thesis]. Tromsø: UiT, The Arctic University of Norway; 2011. 98 p.

31. Knutsen G. Cartilage repair: the use of chondrocytes and bone-marrow cells in cartilage repair [Doctorial thesis]. Tromsø: UiT - The Arctic University of Norway; 2008. 95 p.

32. Mithoefer K, McAdams T, Williams RJ, Kreuz PC, Mandelbaum BR. Clinical efficacy of the microfracture technique for articular cartilage repair in the knee: an evidence-based systematic analysis. American Journal of Sports Medicine. 2009 Oct;37(10):2053-63.

33. Karlsen TA. In vitro chondrogenesis: the role of microRNAs during differentiation and dedifferentiation [Doctorial thesis]. Oslo: University of Oslo (Faculty of Medicine) 2013. 162 p.

34. Cartilage repair and regeneration [Internet] Singapore: Pinnacle Orthopaedic Group, Mount Elizabeth Medical Centre; 2016 [cited 2016 04.10]. Available from: http://p-ortho.com/knee-services/cartilage-repair-and-regeneration/.

35. Alberts B, Wilson JH, Hunt T. Specialized Tissues, Stem Cells, and Tissue Renewal. In: Anderson M, Granum S, editors. Molecular Biology of the Cell. 5th ed. New York, USA: Garland Science; 2008. p. 1417.

36. Randall MD. Human embryology. In: Randall MD, editor. Medical Sciences at a Glance. At a Glance. Hoboken: Wiley-Blackwell; 2013. p. 116-7.

37. Mummery C, Wilmut I, van de Stolpe A, A.J. Roelen B. What are stem cells? In: Mummery C, Wilmut I, van de Stolpe A, A.J. Roelen B, editors. Stem cells: scientific facts and fiction. Amsterdam: Elsevier; 2011. p. 45-58.

38. Ding DC, Chang YH, Shyu WC, Lin SZ. Human umbilical cord mesenchymal stem cells: a new era for stem cell therapy. Cell Transplantation. 2015 Jan;24(3):339-47.

39. Wei X, Yang X, Han ZP, Qu FF, Shao L, Shi YF. Mesenchymal stem cells: a new trend for cell therapy. Acta Pharmacologica Sinica. 2013 Jun;34(6):747-54.

40. Wakao S, Akashi H, Kushida Y, Dezawa M. Muse cells, newly found non-tumorigenic pluripotent stem cells, reside in human mesenchymal tissues. Pathology International. 2014 Jan;64(1):1-9.

41. Islam A, Hansen AK, Mennan C, Martinez I. Mesenchymal stromal cells from human umbilical cords display poor chondrogenic potential in scaffold-free three dimensional cultures. European Cells & Materials. In press. 2016.

42. Leijten JC, Georgi N, Wu L, van Blitterswijk CA, Karperien M. Cell sources for articular cartilage repair strategies: shifting from monocultures to cocultures. Tissue Engineering Part B: Reviews. 2013 Feb;19(1):31-40.

43. Ioan-Facsinay A, Kloppenburg M. An emerging player in knee osteoarthritis: the infrapatellar fat pad. Arthritis Research & Therapy. 2013 Dec;15(6):225.

44. Peng L, Jia Z, Yin X, Zhang X, Liu Y, Chen P, et al. Comparative analysis of mesenchymal stem cells from bone marrow, cartilage, and adipose tissue. Stem Cells and Development. 2008 Aug;17(4):761-73.

45. Lee SY, Nakagawa T, Reddi AH. Mesenchymal progenitor cells derived from synovium and infrapatellar fat pad as a source for superficial zone cartilage tissue engineering: analysis of superficial zone protein/lubricin expression. Tissue Engineering Part A. 2010 Jan;16(1):317-25.

46. Wickham MQ, Erickson GR, Gimble JM, Vail TP, Guilak F. Multipotent stromal cells derived from the infrapatellar fat pad of the knee. Clinical Orthopaedics and Related Research. 2003 Jul(412):196-212.

47. López-Ruiz E, Perán M, Cobo-Molinos J, Jiménez G, Picón M, Bustamante M, et al. Chondrocytes extract from patients with osteoarthritis induces chondrogenesis in infrapatellar fat pad-derived stem cells. Osteoarthritis and Cartilage. 2013 Jan;21(1):246-58.

48. El Omar R, Beroud J, Stoltz JF, Menu P, Velot E, Decot V. Umbilical cord mesenchymal stem cells: the new gold standard for mesenchymal stem cell-based therapies? Tissue Engineering Part B: Reviews. 2014 Oct;20(5):523-44.

49. Majore I, Moretti P, Stahl F, Hass R, Kasper C. Growth and differentiation properties of mesenchymal stromal cell populations derived from whole human umbilical cord. Stem Cell Reviews. 2011 Mar;7(1):17-31.

50. What Is Cord Lining? [Internet] Kuala Lumpur, Malaysia: StemLife Berhad; 2016 [cited 2016.04.01]. Available from: http://stemlife.com/stemlife/cord-tissue/what-is-cord-lining.

51. Sharony R, Keltz E, Biron-Shental T, Kidron D. Morphometric characteristics of the umbilical cord and vessels in fetal growth restriction and pre-eclampsia. Early Human Development. 2016 Jan;92:57-62.

52. Kuroda Y, Kitada M, Wakao S, Nishikawa K, Tanimura Y, Makinoshima H, et al. Unique multipotent cells in adult human mesenchymal cell populations. Proceedings of the National Academy of Sciences of the United States of America. 2010 Mar;107(19):8639-43.

53. Wakao S, Kuroda Y, Ogura F, Shigemoto T, Dezawa M. Regenerative Effects of Mesenchymal Stem Cells: Contribution of Muse Cells, a Novel Pluripotent Stem Cell Type that Resides in Mesenchymal Cells. Cells. 2012 Nov;1(4):1045-60.

54. Wakao S, Kitada M, Kuroda Y, Shigemoto T, Matsuse D, Akashi H, et al. Multilineage-differentiating stress-enduring (Muse) cells are a primary source of induced pluripotent stem cells in human fibroblasts. Proceedings of the National Academy of Sciences of the United States of America. 2011 Jun;108(24):9875-80.

55. Kuroda Y, Wakao S, Kitada M, Murakami T, Nojima M, Dezawa M. Isolation, culture and evaluation of multilineage-differentiating stress-enduring (Muse) cells. Nature Protocols. 2013 Jun;8(7):1391-415.

56. Tsuchiyama K, Wakao S, Kuroda Y, Ogura F, Nojima M, Sawaya N, et al. Functional melanocytes are readily reprogrammable from multilineage-differentiating stress-enduring (muse) cells, distinct stem cells in human fibroblasts. Journal of Investigative Dermatology. 2013 Oct;133(10):2425-35.

57. Heneidi S, Simerman AA, Keller E, Singh P, Li X, Dumesic DA, et al. Awakened by Cellular Stress: Isolation and Characterization of a Novel Population of Pluripotent Stem Cells Derived from Human Adipose Tissue. PloS One. 2013 Jun;8(6):e64752.

58. Dulbecco's Modified Eagle's Medium (high glucose) [Internet] St. Louis, USA: Sigma-Aldrich; 2012 [cited 2015.12.08]. Available from: https://www.sigmaaldrich.com/catalog/product/sigma/d5796?lang=en&region=NO.

59. Minimum Essential Medium Eagle [Internet] St. Louis, USA: Sigma-Aldrich; 2012 [cited 2015.12.08]. Available from: http://www.sigmaaldrich.com/life-science/cell-culture/classical-media-salts/mem-media.html#for%20more%20information.

60. GlutaMax Media [Internet] Waltham, Massachusetts, USA: Thermo Fisher Scientific; 2015 [cited 2015.11.24]. Available from: http://www.thermofisher.com/no/en/home/life-science/cell-culture/mammalian-cell-culture/media-supplements/glutamax-media/glutamax-vs-glutamine.html.

61. Dulbecco's Phosphate Buffered Saline [Internet] St. Louis, USA: Sigma-Aldrich; 2012 [cited 2015.12.08]. Available from: http://www.sigmaaldrich.com/catalog/product/sigma/d8537?lang=en&region=NO.

62. Fetal Bovine Serum [Internet] Darmstadt, Germany: Merck Millipore Corporation; 2015 [cited 2015.12.08]. Available from: http://www.merckmillipore.com/NO/en/product/Fetal-Bovine-Serum%2C-US-Origin,MM_NF-TMS-013-B.

63. Cell Morphology [Internet] Waltham, Massachusetts, USA: Thermo Fisher Scientific; 2015 [cited 2015.12.08]. Available from: https://www.thermofisher.com/no/en/home/references/gibco-cell-culture-basics/cell-morphology.html.

64. Scientific TF. Freezing Cells [Internet] Waltham, Massachusetts, USA: Thermo Fisher Scientific; 2015 [cited 2015.11.26]. Available from: https://www.thermofisher.com/no/en/home/references/gibco-cell-culture-basics/cell-culture-protocols/freezing-cells.html.

65. Andrews PW, Damjanov I, Simon D, Banting GS, Carlin C, Dracopoli NC, et al. Pluripotent embryonal carcinoma clones derived from the human teratocarcinoma cell line Tera-2. Differentiation in vivo and in vitro. Laboratory Investigation. 1984 Feb;50(2):147-62.

66. Sample Preparation Guidelines For Sorts [Internet]: University of Glasgow, The Flow Cytometry Facility; [cited 2015.12.09]. Available from: http://www.gla.ac.uk/media/media_265158_en.pdf.

67. Human Pluripotent Stem Cell Starter Kit Assay Procedure [Internet] Minneapolis, USA: R&D Systems Inc.; 2013 [cited 2016.03.01]. Available from: https://www.rndsystems.com/products/human-pluripotent-stem-cell-starter-kit_sc029#assay-procedure.

68. FACS FAQ [Internet] St. Louis, Missouri, USA: Washington University School of Medicine: Department of Pathology & Immunology; [cited 2015.05.12]. Available from: http://pathology.wustl.edu/research/cores/facs/index.php?page=FACS%20FAQs.

69. Human MSC Analysis Kit [Internet] California: BD Biosciences; 2015 [cited 2016.04.08]. Available from: http://m.bdbiosciences.com/us/applications/research/stem-cell-research/stem-cell-kits-and-cocktails/human/human-msc-analysis-kit/p/562245.

70. Draper JS, Pigott C, Thomson JA, Andrews PW. Surface antigens of human embryonic stem cells: changes upon differentiation in culture. Journal of Anatomy. 2002 Mar;200(3):249-58.

71. Achilli T-M, Meyer J, Morgan JR. Advances in the formation, use and understanding of multi-cellular spheroids. Expert Opinion on Biological Therapy. 2012 Oct;12(10):1347-60.

72. Poly(2-hydroxyethyl methacrylate) [Internet] St. Louis, USA: Sigma-Aldrich; 2012 [cited 2015.12.08]. Available from: http://www.sigmaaldrich.com/catalog/product/sigma/p3932?lang=en&region=NO.

73. Yang ZX, Han ZB, Ji YR, Wang YW, Liang L, Chi Y, et al. CD106 identifies a subpopulation of mesenchymal stem cells with unique immunomodulatory properties. PloS One. 2013 Mar;8(3):e59354.

74. Wang L, Tran I, Seshareddy K, Weiss ML, Detamore MS. A comparison of human bone marrow-derived mesenchymal stem cells and human umbilical cord-derived mesenchymal stromal cells for cartilage tissue engineering. Tissue Engineering Part A. 2009 Aug;15(8):2259-66.

75. Ibrahim AM, Elgharabawi NM, Makhlouf MM, Ibrahim OY. Chondrogenic differentiation of human umbilical cord blood-derived mesenchymal stem cells in vitro. Microscopy Research and Technique. 2015 Aug;78(8):667-75.

76. Zhang X, Hirai M, Cantero S, Ciubotariu R, Dobrila L, Hirsh A, et al. Isolation and characterization of mesenchymal stem cells from human umbilical cord blood: reevaluation of critical factors for successful isolation and high ability to proliferate and differentiate to chondrocytes as compared to mesenchymal stem cells from bone marrow and adipose tissue. Journal of Cellular Biochemistry. 2011 Apr;112(4):1206-18.

77. Park YB, Song M, Lee CH, Kim JA, Ha CW. Cartilage repair by human umbilical cord blood-derived mesenchymal stem cells with different hydrogels in a rat model. Journal of Orthopaedic Research. 2015 Nov;33(11):1580-6.

78. Simerman AA, Perone MJ, Gimeno ML, Dumesic DA, Chazenbalk GD. A mystery unraveled: nontumorigenic pluripotent stem cells in human adult tissues. Expert Opinion on Biological Therapy. 2014 Jul;14(7):917-29.

79. Simerman AA, Dumesic DA, Chazenbalk GD. Pluripotent muse cells derived from human adipose tissue: a new perspective on regenerative medicine and cell therapy. Clinical and Translational Medicine. 2014 May;3:12.

80. Ogura F, Wakao S, Kuroda Y, Tsuchiyama K, Bagheri M, Heneidi S, et al. Human adipose tissue possesses a unique population of pluripotent stem cells with nontumorigenic and low telomerase activities: potential implications in regenerative medicine. Stem Cells and Development. 2014 Apr;23(7):717-28.

81. Yamauchi T, Kuroda Y, Morita T, Shichinohe H, Houkin K, Dezawa M, et al. Therapeutic Effects of Human Multilineage-Differentiating Stress Enduring (MUSE) Cell Transplantation into Infarct Brain of Mice. PloS One. 2015 Mar;10(3):e0116009.

82. Kinoshita K, Kuno S, Ishimine H, Aoi N, Mineda K, Kato H, et al. Therapeutic Potential of Adipose-Derived SSEA-3-Positive Muse Cells for Treating Diabetic Skin Ulcers. Stem Cells Translational Medicine. 2015 Feb;4(2):146-55.

83. Liu J, Yang Z, Qiu M, Luo Y, Pang M, Wu Y, et al. Developmental potential of cloned goat embryos from an SSEA3(+) subpopulation of skin fibroblasts. Cellular Reprogramming. 2013 Apr;15(2):159-65.

84. Yang Z, Liu J, Liu H, Qiu M, Liu Q, Zheng L, et al. Isolation and characterization of SSEA3(+) stem cells derived from goat skin fibroblasts. Cellular Reprogramming. 2013 Jun;15(3):195-205.

85. Wakao S, Kitada M, Kuroda Y, Dezawa M. Isolation of adult human pluripotent stem cells from mesenchymal cell populations and their application to liver damages. Methods in Molecular Biology. 2012 Nov;826:89-102.

86. Battula VL, Bareiss PM, Treml S, Conrad S, Albert I, Hojak S, et al. Human placenta and bone marrow derived MSC cultured in serum-free, b-FGF-containing medium express cell surface frizzled-9 and SSEA-4 and give rise to multilineage differentiation. Differentiation; research in biological diversity. 2007 Apr;75(4):279-91.

87. Lopa S, Colombini A, Stanco D, de Girolamo L, Sansone V, Moretti M. Donor-matched mesenchymal stem cells from knee infrapatellar and subcutaneous adipose tissue of osteoarthritic donors display differential chondrogenic and osteogenic commitment. European Cells & Materials. 2014 Apr;27:298-311.

88. Abdi R, Fiorina P, Adra CN, Atkinson M, Sayegh MH. Immunomodulation by Mesenchymal Stem Cells : A Potential Therapeutic Strategy for Type 1 Diabetes. Diabetes. 2008 Jul;57(7):1759-67.

89. Ankrum JA, Ong JF, Karp JM. Mesenchymal stem cells: immune evasive, not immune privileged. Nature Biotechnology. 2014 Mar;32(3):252-60.

90. Arzi B, DuRaine GD, Lee CA, Huey DJ, Borjesson DL, Murphy BG, et al. Cartilage immunoprivilege depends on donor source and lesion location. Acta Biomaterialia. 2015 Sep;23:72-81.

91. Playfair JHL, Chain BM. CD classification. In: Immunology at a glance. 10th ed. Chichester, West Sussex: Wiley-Blackwell; 2013. p. 113-4.

92. CD44 [Internet] Barcelona, Spain: HCDM (Human Cell Differentiation Molecules); 2013 [cited 2016.04.15]. Available from: http://www.hcdm.org/index.php?option=com_molecule&cdnumber=CD44.

93. CD90 [Internet] Barcelona, Spain: HCDM (Human Cell Differentiation Molecules); 2013 [cited 2016.04.15]. Available from: http://www.hcdm.org/index.php?option=com_molecule&cdnumber=CD90.

94. CD73 [Internet] Barcelona, Spain: HCDM (Human Cell Differentiation Molecules); 2013 [cited 2016.04.15]. Available from: http://www.hcdm.org/index.php?option=com_molecule&cdnumber=CD73.

95. CD105 [Internet] Barcelona, Spain: HCDM (Human Cell Differentiation Molecules); 2013 [cited 2016.04.15]. Available from: http://www.hcdm.org/index.php?option=com_molecule&cdnumber=CD105.

96. CD106 [Internet] Barcelona, Spain: HCDM (Human Cell Differentiation Molecules); 2013 [cited 2016.04.15]. Available from: http://www.hcdm.org/index.php?option=com_molecule&cdnumber=CD106.

97. CD146 [Internet] Barcelona, Spain: HCDM (Human Cell Differentiation Molecules); 2013 [cited 2016.04.15]. Available from: http://www.hcdm.org/index.php?option=com_molecule&cdnumber=CD146.

98. CD166 [Internet] Barcelona, Spain: HCDM (Human Cell Differentiation Molecules); 2013 [cited 2016.04.15]. Available from: http://www.hcdm.org/index.php?option=com_molecule&cdnumber=CD166.

99. Stem Cell Markers [Internet] Minneapolis, USA: RnD Systems Inc.; 2003 [cited 2016.04.15]. Available from: https://www.rndsystems.com/resources/articles/stem-cell-markers#EmbryonicStemCellMarkers.

100. Human Integrin beta 1/CD29 Antibody [Internet] Minneapolis, USA: R&D Systems; 2015 [cited 2016.05.12]. Available from: https://www.rndsystems.com/products/human-integrin-beta1-cd29-antibody-p5d2_mab17781.

101. Recombinant Human CD44 Fc Chimera Protein, CF [Internet] Minneapolis, USA: R&D Systems; 2015 [cited 2016.05.12]. Available from: https://www.rndsystems.com/products/recombinant-human-cd44-fc-chimera-protein-cf_3660-cd#product-details.

102. Recombinant Human 5'-Nucleotidase/CD73 Protein, CF [Internet] Minneapolis, USA: R&D Systems; 2016 [cited 2016.05.12]. Available from: https://www.rndsystems.com/products/recombinant-human-5-nucleotidase-cd73-protein-cf_5795-en#product-details.

Appendices

Appendix A – The explant culture procedure

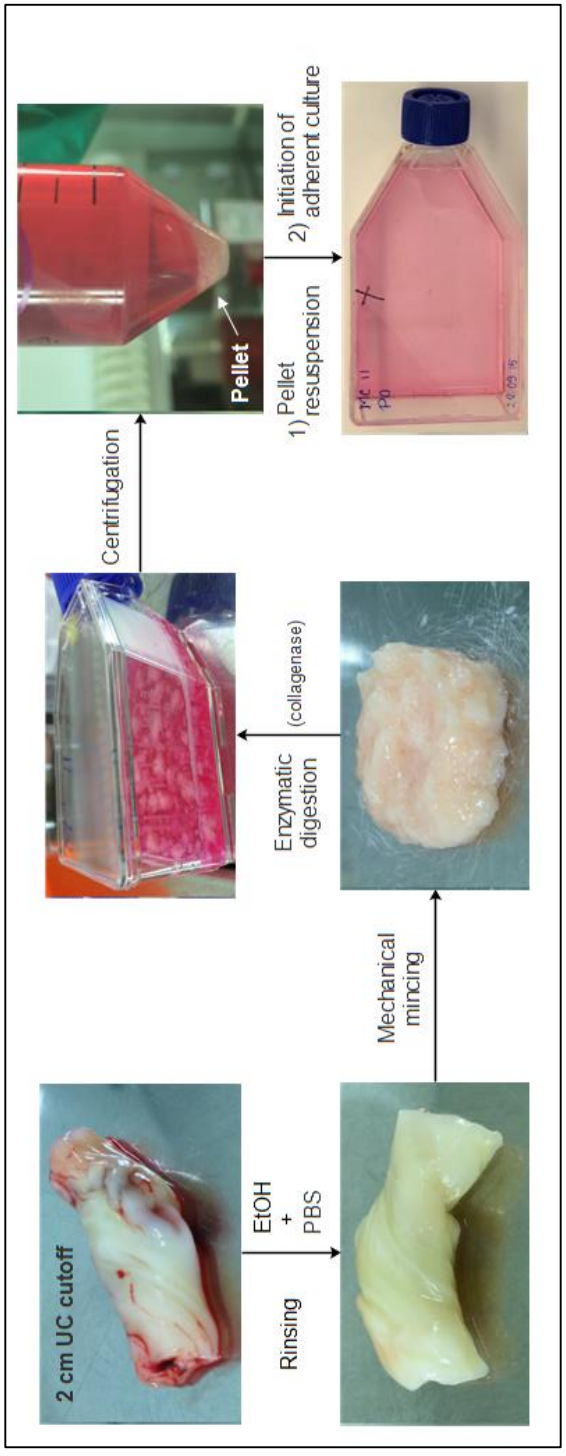

Figure 29. Schematically presentation of the explant culture procedure. An umbilical cord section is rinsed in PBS and EtOH to remove blood and reduce the risk of contamination. Mechanical mincing and enzymatic digestion is carried out, followed by centrifugation. The pellet is further resuspended and planted in a culturing flask with medium + 20 % FBS. The procedure was carried out the same way for Hoffa's Fat Pad. Picture made by using the software Edraw Max 7.9 (17.04.16).

Appendix B – Clusters of differentiation

Overview of surface markers (clusters of differentiation)

Table 6. Clusters of differentiation (CDs) and embryonic markers. The table show common MSC and MUSE-cell markers compared to our analytical findings in MC-MSCs and MC-MUSE-cells. CD105 is a multipotency marker, commonly expressed on both MSCs and MUSE-cells. SSEA-3 is an embryonic stem cell marker expressed on pluripotent stem cells like MUSE-cells. The markers SSEA-3 and -4 are not a part of the "CD"-family, even if they are presented in this way here. Description, function and distribution information adapted from (91-102). A question mark points out characteristics that is not fully understood.

CD	*Description*	*Function*	*Distri-bution*	*Antibody used*	*MSCs**	*MUSE-cells**
CD29	β1-integrin	Adhesion, Apoptosis, Differentiation	-	-	+/NA	+/NA
CD44	Homing cell adhesion molecule (HCAM) (Indian blood group system)	Adhesion, Costimulation, Homing, Cell growth, Cell migration, Hyaluronan receptor	T, B, M, DC, G	PE Mouse Anti-Human CD44	+/+	÷/NA
CD90	Thy 1	Haemopoiesis	T, B, E	FITC Mouse Anti-Human CD90	+/+	+/NA
CD73	Ecto-5'-nucleotidase (isoenzyme)	Production of extracellular adenosine. Involved in responses of inflamm. and tissue injury.	B	APC Mouse Anti-Human CD73	+/+	÷/NA
CD105	Endoglin	TGF-coreceptor	E	PerCP-Cy™5.5 Mouse Anti-Human CD105	+/+	+/NA
CD106	Vascular cell adhesion molecule 1 (VCAM-1)	Adhesion	E	PE Mouse Anti-Human CD106	+/÷ (**)	÷/NA
CD146	Melanoma cell adhesion molecule (MCAM)	Adhesion?		PE Mouse Anti-Human CD146	+/+	÷/NA
CD166	Activated leukocyte cell adhesion molecule (ALCAM)	Adhesion	T, B, E	PE Mouse Anti-Human CD166	+/+	÷/NA
SSEA-3	-	Control cell-surface interactions during development?	-	Anti-Stage-Specific Embryonic Antigen-3 Antibody	÷/NA	+/+
SSEA-4	-	(see SSEA-3)	-	Anti-Stage-Specific Embryonic Antigen-4 Antibody	÷/NA	÷/+

**(Expected/Discovered in our analysis)*

***Weakly $CD106^{+}$ in our findings*

Abbreviations
B = B cells, DC = Dendritic cells, E = Endothelium, G = Granulocyte, M = Monocyte/macrophage, T = T cells, NA = Not added

Appendix C – MUSE protocol

Protocol for characterization/sorting of MUSE cells

1. Cells are ready to be passaged upon ~100 % confluency. Keep trypsin and necessary medium in the oven. Keep the antibodies in room temperature.
2. Dissociate the cells from the culture plate (N.B.: if high confluency – add 6-8 ml Enzyme Free and wait 15-25 min + 5 min trypsin).
3. Centrifuge at 400 G for 3 minutes (37 °C).
4. Prepare 1 tube of 30 ml FACS buffer for each cell culture (do this when waiting for the cells to detach).
5. Resuspend the cells in medium for counting. Use a cell strainer.
6. Count cells.
7. Wash cells in 2-3 ml FACS buffer followed by centrifugation (400 G for 3 minutes). Do this twice.
8. Reduce unspecific antibody-binding by adding a few ml of PBS + HSA (10 %) for 20 minutes.
9. Wash cells in 2-3 ml FACS buffer followed by centrifugation (400 G for 3 minutes). Do this twice.
10. Resuspend the cells in FACS buffer to a concentration of 1-5 x 10^6 cells/ml.
11. Label tubes 1-5.
12. Transfer 100 µl of prepared cell suspension (< 1 x 10^6 cells/100 µl) to tube 1-5.
13. Add *primary antibodies* (AB) to tube 4 and 5 (4 µl for SSEA-3 and 2 µl for SSEA-4).
14. Incubate the tubes on ice and in the dark for 1 hour and **GENTLY** pipette up/down every 10 minutes.
15. Wash cells twice w/FACS buffer and centrifuge at 400 G for 3 min. Resuspend the cells. Do this twice.
16. Resuspend the cells in 99 µl FACS buffer.
17. Add *secondary antibodies* (AB) to tube 2-5 (1 µl of both) and repeat step 14 and 15.
18. Resuspend the cells in 300 µl of FACS buffer.
19. Transfer the cells to appropriate tubes for flow cytometry and label them 1-5.
20. Fill 1 ml medium in an extra tube for collecting of MUSE cells (only if sorting, not characterization).
21. Collect cells for MUSE cell culture from tube 3 (if sorting is carried out).

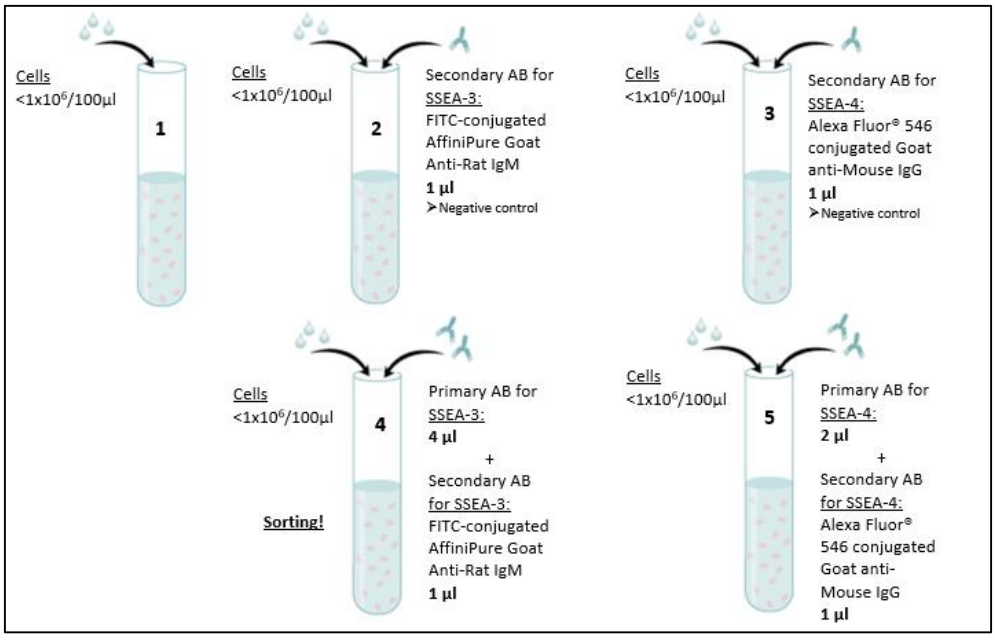

Figure 30. Overview of the setup for analysis of MUSE-cells by flow cytometry. Images adapted and modified from (67). Protocol based on recommendation from (55).

Notes of importance
Step number 2, 8, 14 and 17 in the procedure are **time-consuming**. Allocation of sufficient time for sample preparations should therefore be done. In this study, 5-7 hours went to sample preparation before running flow cytometry. A 50 µl pipette is suitable for mixing (step 14).

Appendix D – MUSE-differentiation *in vivo* and *in vitro*

Table 7. MUSE-cell studies *in vivo* and *in vitro*. *In vivo* studies were carried out in immunodeficient mice. MUSE-cell migration (*in vivo*) is often confirmed by using green fluorescent protein (GFP)-labeling. Each of the three lineages (endoderm, ectoderm and mesoderm) are represented (not shown), indicating that MUSE-cells can undergo triploblastic differentiation, *in vivo* and *in vitro*. MUSE-cells has, practically speaking, been applied in humans (*in vivo*), as a part of MSC populations (40, 53). Information adapted from (52-54, 56, 57, 81, 82).

In vivo	*Description*	*In vitro*	*Description*
Skin damage (52, 53)	Local injection with integration into damaged skin. Expression of cytokeratin 14 (52). Peripheral injection, with integration in the skin, and differentiation into keratinocytes (cytokeratin 14 positive) (53)	*M-cluster transferred to gelatin-coated dishes (52, 56)*	Cells positive for neurofilament-M (ectoderm), α-smooth muscle actin (mesoderm), α-fetoprotein (endoderm), cytokeratin 7 (endoderm) or desmin (mesoderm). 1st and 3rd generation M-clusters expressed α-fetoprotein and GATA6 (endoderm), MAP-2 (ectoderm), and Nkx2.5 (mesoderm).
Autologous transplantation of melanocytes (56)	3D skin cultures with melanocyte-differentiated MUSE-cells (medium induced differentiation) transplanted onto back skin of mice. The cells homed to the basal layer of epidermis, where they produced melanin which was further delivered to keratinocytes.	*Melanocyte differentiation (56)*	*Medium induced melanocyte differentiation:* Morphology similar to human melanocytes after 6 weeks, with expression of melanocyte-related markers. Positive L-DOPA reaction assay suggests melanin production. *3D skin cultures with MUSE:* Pigmented cells with melanocyte markers and melanin production observed migrated to the epidermis basal layer after 15 days. Induced diff.
Gastrocnemius muscle (52)	Intravenous (i.v.) injection with integration in regenerating muscle. Cells appeared as mature myofibers after 4 weeks, expressing human dystrophin.	*Myocyte-like cells(57)*	*Myocyte induction:* Cells with a characteristic morphology, expression of SMA.
Skeletal muscle degeneration (53)	I.v. injection (peripheral bloodstream) with differentiation into skeletal muscle cells (positive for human dystrophin).	*Adipocyte-like cells (54, 57)*	*Adipocyte induction:* Cells with lipid droplets
Liver damage (52, 53)	I.v. injection with integration in the liver. After 4 weeks, cells expressed human albumin and human antitrypsin.	*Hepatocyte- and biliary-like cells (54, 57)*	*Hepatocyte induction:* Cells expressing human α-fetoprotein and human albumin (54). Pan keratin and cytokeratin 7 also reported (57)
Spinal cord injury (53)	I.v. injection (peripheral bloodstream) with differentiation into neuronal cells and integration in spinal cord (positive for neurofilament).	*Neural-like cells (54, 57)*	*Neuronal differentiation medium:* Generation of spheres positive for neural stem cell markers (nestin, Musashi and NeuroD [Glut-R also reported]). Further differentiation yielded cells with more neuron-like morphology, being nestin+ and MAP-2+ or GFAP+.
Infarct brain (81)	Transplantation into the ipsilateral striatum in infarct mice brain, with integration in peri-infarct cortex and differentiation into Tuj-1- and NeuN-expressing cells (neural-like cells).		
Testes (52)	MUSE-cells (MEC) or M-clusters injected into testes. No teratoma formation seen, even after 6 months.	*Osteoblast-like cells (54)*	*Osteoblast induction:* Osteocalcin-positive cells.

Table 7 continued:

In vivo	*Description*	*In vitro*	*Description*
Diabetic skin ulcers (82)	Induction of skin ulcers in mice with type 1 diabetes vs. non-diabetic mice. Diabetic mice had the slowest wound healing. MUSE-rich vs. MUSE-poor populations were compared. Cells were injected into the subcutis, locally to the wound. MUSE-cells integrated in dermis (w/differentiation to vascular endothelial cells, among others) and yielded accelerated wound healing, compared to the control groups.		